Molecular Biology of the Cell
Vol. 16, 3642–3658, August 2005

EHD Proteins Associate with Syndapin I and II and Such Interactions Play a Crucial Role in Endosomal Recycling[D]

Anne Braun,*† Roser Pinyol,*† Regina Dahlhaus,* Dennis Koch,* Paul Fonarev,‡ Barth D. Grant,‡ Michael M. Kessels,* and Britta Qualmann*

*Department of Neurochemistry and Molecular Biology, Leibniz Institute for Neurobiology, D-39118 Magdeburg, Germany; and ‡Department of Molecular Biology and Biochemistry, Rutgers University, Piscataway, NJ 08854

Submitted January 28, 2005; Revised April 19, 2005; Accepted May 23, 2005
Monitoring Editor: Howard Riezman

EHD proteins were shown to function in the exit of receptors and other membrane proteins from the endosomal recycling compartment. Here, we identify syndapins, accessory proteins in vesicle formation at the plasma membrane, as differential binding partners for EHD proteins. These complexes are formed by direct eps15-homology (EH) domain/asparagine proline phenylalanine (NPF) motif interactions. Heterologous and endogenous coimmunoprecipitations as well as reconstitutions of syndapin/EHD protein complexes at intracellular membranes of living cells demonstrate the in vivo relevance of the interaction. The combination of mutational analysis and coimmunoprecipitations performed under different nucleotide conditions strongly suggest that nucleotide binding by EHD proteins modulates the association with syndapins. Colocalization studies and subcellular fractionation experiments support a role for syndapin/EHD protein complexes in membrane trafficking. Specific interferences with syndapin–EHD protein interactions by either overexpression of the isolated EHD-binding interface of syndapin II or of the EHD1 EH domain inhibited the recycling of transferrin to the plasma membrane, suggesting that EH domain/NPF interactions are critical for EHD protein function in recycling. Consistently, both inhibitions were rescued by co-overexpression of the attacked protein component. Our data thus reveal that, in addition to a crucial role in endocytic internalization, syndapin protein complexes play an important role in endocytic receptor recycling.

INTRODUCTION

The endocytic pathway is essential for the delivery of membrane components, receptor-bound ligands, and soluble molecules to different intracellular organelles. It requires the concentration of cargo molecules, the formation and detachment of transport vesicles from donor compartments, and the subsequent fusion with proper target compartments. The formation of vesicles is driven by the assembly of specific coat proteins that work in conjunction with additional accessory and regulatory machinery. The most well characterized process is the formation of clathrin-coated vesicles. The proper formation and fission of clathrin-coated pits from the plasma membrane requires the large GTPase dynamin and many accessory proteins. Their functions include, but are certainly not limited to, vesicle size control, bending of the membrane, which may help in the invagination process, and vesicle uncoating (Slepnev and De Camilli, 2000).

Additionally, this complex machinery is connected with the cortical actin cytoskeleton, which may support vesicle formation by different means (Qualmann *et al*., 2000; Qualmann and Kessels, 2002). Syndapins, a family of proteins also referred to as PACSINs, were suggested to be molecular links between membrane trafficking and cortical cytoskeleton dynamics, because syndapins associated with both dynamin and N-WASP, a potent stimulator of the Arp2/3 complex actin polymerization machinery (Qualmann *et al*., 1999; Kessels and Qualmann, 2004). Both functions are supported by in vivo data, the dynamin-binding syndapin Src homology 3 (SH3) domain is a potent inhibitor of receptor-mediated endocytosis and overexpression of full-length syndapin induces numerous filopodia, actin-rich protrusions of the plasma membrane, in an Arp2/3-complex dependent manner (Qualmann and Kelly, 2000). Local actin polymerization has been observed at endocytic sites (Merrifield *et al*., 2002) and coincides with the transient recruitment of the Arp2/3 complex and N-WASP (Merrifield *et al*., 2004). Dominant-negative experiments and in vivo reconstitutions strongly suggested that the role of N-WASP in endocytosis involves the syndapin association and that syndapin-mediated actin polymerization supports clathrin-coated vesicle detachment and movement away from the plasma membrane (Kessels and Qualmann, 2002).

After endocytic internalization, most membrane proteins and lipids return to the plasma membrane after passing through one or several endosomal compartments, such as the sorting endosome and the endocytic recycling compart-

This article was published online ahead of print in *MBC in Press* (http://www.molbiolcell.org/cgi/doi/10.1091/mbc.E05–01–0076) on June 1, 2005.

[D] The online version of this article contains supplemental material at *MBC Online* (http://www.molbiolcell.org).

† These authors contributed equally to this work.

Address correspondence to: Britta Qualmann (qualmann@ifn-magdeburg.de).

Abbreviations used: ERC, endocytic recycling compartment; EH, eps15-homology; NPF, asparagine proline phenylalanine; NPV, asparagine proline valine; NPF***, NPF-to-NPV triple mutant; SH3, Src homology 3.

© 2005 by The American Society for Cell Biology

ment (ERC) (Maxfield and McGraw, 2004). Transport from the ERC, which is a long-lived compartment, also requires the formation of transport vesicles. The machinery needed for the formation of such vesicles or tubules from the ERC is only beginning to be elucidated. The ERC may use mechanisms similar to those used for the formation of transport vesicles from other organelles. In particular, clathrin and dynamin can be found on endosomes (Stoorvogel *et al*., 1996; van Dam *et al*., 2002), implying that they may serve functions there similar to their well studied roles at the plasma membrane.

Proteins that specifically regulate transport from the ERC include the small GTPase Rab11 (Chen *et al*., 1998; Ren *et al*., 1998) and EHD1 (Lin *et al*., 2001). In mammals, EHD1 belongs to a family of four highly related proteins (EHD1–4) (Mintz *et al*., 1999; Pohl *et al*., 2000) that share a very similar domain structure with an N-terminal P-loop–containing nucleotide binding domain, a central region predicted to form coiled coils and a C-terminal Eps15-homology (EH) domain. The *Caenorhabditis elegans* homologue RME-1 was identified in a genetic screen for mutants defective in the receptor-mediated endocytosis of yolk protein. Closer examination of *rme-1* mutants indicated that a block in endocytic recycling was the primary defect (Grant *et al*., 2001). The expression of a mRme-1/EHD1 G429R mutant, designed by analogy to a dominant *C. elegans* mutant (G459R), resulted in the redistribution of the ERC in mammalian cells and slowed the recycling of transferrin receptors (Lin *et al*., 2001), of major histocompatibility complex class I molecules (Caplan *et al*., 2002), the cystic fibrosis transmembrane conductance regulator (Picciano *et al*., 2003) and α-amino-3-hydroxy-5-methyl-4-isoxazolepropionic acid (AMPA)-type glutamate receptors (Park *et al*., 2004) back to the cell surface. Depletion of mRme-1/EHD1 by RNA interference confirmed the role of mRme-1/EHD1 in mammalian cell protein recycling to the cell surface (Naslavsky *et al*., 2004). Here, we identify EHD proteins as differential interaction partners of syndapins. We examine the molecular requirements for these interactions as well as means of regulation. Furthermore, we demonstrate that the ability of mRme-1/EHD1 to form protein complexes through EH domain/asparagine proline phenylalanine (NPF) interactions is crucial for the recycling process.

MATERIALS AND METHODS

DNA Constructs and Recombinant Proteins

Constructs coding for glutathione *S*-transferase (GST)-fusion proteins of syndapin I, syndapin I ΔSH3, and the short and long splice variants of syndapin II and for a maltose-binding protein (MBP)-fusion protein of syndapin I ΔSH3 were described previously (Qualmann *et al*., 1999; Qualmann and Kelly, 2000). Further GST-fusion proteins, such as syndapin I SH3 domain (aa 378–441), syndapin II SH3 domain (aa 422–488), and the NPF motif regions of syndapin I (aa 336–386), syndapin II-s (aa 338–387), and syndapin II-l (aa 338–428) were generated by PCR on appropriate templates and cloning into pGEX vectors. Mammalian expression constructs encoding green fluorescent protein (GFP) or FLAG-tagged syndapins and fragments thereof were generated by subcloning into pEGFP-C1 (BD Biosciences Clontech, Palo Alto, CA) and pCMV-Tag2B (Stratagene, La Jolla, CA), respectively. Xpress-tagged syndapin II-l and syndapin II-l ΔSH3 were described in Qualmann and Kelly (2000). For yeast two-hybrid analyses, syndapin I full-length and syndapin I ΔSH3 were inserted into the pGBTK7 vector. The plasmid encoding mitochondria-targeted full-length syndapin I was described in Kessels and Qualmann (2002). Point mutations in the NPF motifs of syndapin I and II-l, resulting in the exchange of phenylalanine to valine, were introduced by site-directed mutagenesis via PCR. Syndapin III was amplified by PCR from a rat retina library (Seidenbecher *et al*., 2004) and cloned into *Eco*RI-*Sal*I sites of pGEX-5X-1 (Amersham Biosciences, Piscataway, NJ).

GST-mRme-1/EHD1 full-length and GST-EH domain (aa 408–534) expression constructs were created by PCR with full-length mRme-1/EHD1 as template and cloned into pGEX-2T. Full-length FLAG-mRme-1/EHD1, EGFP-mRme-1/EHD1 wild-type, G65R, and G429R constructs were described previously (Lin *et al*., 2001). The W485A mutation was engineered into the full-length EGFP-mRme-1/EHD1 construct using appropriate mutation primers according to manufacturer's instructions (QuikChange XL; Stratagene).

Mouse EHD2, EHD3, and EHD4 were amplified from expressed sequence tag clones (RZPD) IMAGp998G059315Q3, IMAGp998H2413737Q3, and IMAGp998A058521Q3, respectively, and subcloned into pCMV-Tag2 (Stratagene), pEGFP-C (BD Biosciences Clontech), and pGEX (Amersham Biosciences) vectors. The partial yeast two-hybrid clone of EHD3 (aa 367–535) was subcloned into pGEX-4T2. The EH domain of mRme-1/EHD1 was subcloned into pEGFP-C1 (BD Biosciences Clontech) and into a derivative of our mitochondrial targeting vector (Kessels and Qualmann, 2002), Mito-GFP vector, that was generated by inserting the green fluorescent protein (GFP) sequence between the FLAG-tag and the multiple cloning site. Constructs encoding for GST-Eps15 EH (encompassing all three EH domains) and GST-Intersectin EH (encompassing EH domains a and b) were from Brian Kay (Argonne National Laboratory, Chicago, IL). The bacterial expression vector permitting the expression of *C. elegans* Rme-1 as a GST-fusion protein has been described previously (Lee *et al*., 2005). All PCR-amplified DNAs were verified for integrity by sequencing.

GST- and MBP-fusion proteins were expressed and purified as described previously (Qualmann *et al*., 1999; Kessels *et al*., 2000).

Antibodies

Rabbit anti-syndapin I and anti-syndapin II antibodies, guinea pig anti-syndapin II antibodies (antisera 2521, 2704, and P339) and anti-GST antibodies were described previously (Qualmann *et al*., 1999; Qualmann and Kelly, 2000).

Polyclonal anti-syndapin I antibodies were raised in guinea pig (Pineda Antikörper-Service, Berlin, Germany) against a purified GST-fusion protein of amino acid residues 1–382 of rat syndapin I. Antibodies were affinity purified on GST and MBP-syndapin I (aa 1–382) blotted to nitrocellulose membranes.

Polyclonal anti-mRme/EHD antibodies were raised in rabbit (Covance Immunological Services, Princeton, NJ) against a synthetic peptide (CADLP-PHLVPPSKRRHE), corresponding to the extreme C terminus of the mouse Rme-1/EHD1 protein, conjugated to keyhole limpet hemocyanin. Antisera raised against this peptide were affinity purified against immobilized antigenic peptide (Sulfolink kit) according to the manufacturer's instructions (Pierce Chemical, Rockford, IL). Due to high sequence conservation, the antibodies also recognize the EHD protein isoforms 3 and 4 relatively well (Figure S1) and work for several species, such as mouse, rat, and human.

Monoclonal anti-FLAG (M2) and anti-synaptophysin antibodies were from Sigma (St. Louis, MO), monoclonal anti-GFP (B34) antibodies were from BAbCO (Richmond, CA), monoclonal anti-TGN38 antibodies were from BD Transduction Laboratories (Lexington, KY), and monoclonal anti-Xpress antibodies were from Invitrogen (Carlsbad, CA).

Secondary antibodies used include goat anti-mouse peroxidase and goat anti-rabbit peroxidase from Dianova (Hamburg, Germany); goat anti-guinea pig peroxidase and fluorescein isothiocyanate (FITC) goat anti-guinea pig from MP Biomedicals (Irvine, CA); and Alexa Fluor 488 goat anti-mouse, Alexa Fluor 568 goat anti-mouse, Alexa Fluor 568 goat anti-rabbit, Alexa Fluor 647 goat anti-mouse, and Alexa Fluor 647 goat anti-rabbit from Molecular Probes (Eugene, OR).

Blot Overlay and Coprecipitation Assays

Coprecipitations of rat brain proteins with immobilized GST-fusion proteins were performed with rat brain extracts containing 10 mM (Figure 1E) or 150 mM NaCl according to Qualmann and Kelly (2000) and Qualmann *et al*. (2004). Bound proteins were separated on SDS-PAGE, blotted to nitrocellulose, and probed with anti-syndapin I (2704) or anti-EHD antibodies.

Coprecipitations from lysates of transfected human embryonic kidney (HEK)293 cells were essentially performed as described previously (Kessels *et al*., 2001; Kessels and Qualmann, 2002).

Blot overlay experiments were performed with recombinant GST-mRme-1/EHD1 EH domain and GST on extracts from HEK293 cells transfected with GFP or GFP-syndapin II-l according to the procedure described previously (Kessels and Qualmann, 2002).

Tissue Fractionation

Tissue fractionation was carried out essentially as described in Qualmann *et al*. (2004). In brief, rat brain cortices and hippocampi were homogenized in 320 mM sucrose, 5 mM HEPES, pH 7.4. The homogenate was centrifuged at 1000 × *g* to remove cell debris and nuclei, and the resulting low-speed supernatant (S1) was recentrifuged at 12,000 × *g* for 15 min. While the obtained supernatant S2 was further fractionated by centrifugation at 100,000 × *g* for 1 h, yielding a microsomal pellet (PM) and a ultrahigh-speed supernatant (SM), the resulting pellet P2 (crude membrane fraction) was loaded onto a sucrose step gradient (0.85/1.0/1.2 M). Myelin, light membranes, and synaptosomes were isolated at the different sucrose interfaces. The mitochondria- and heavy-membrane–containing fraction (mitochondria) was obtained as pellet. Synaptosomal membranes were isolated after the osmotic lysis of synaptosomes in 1 mM Tris/HCl, pH 8.1, for 30 min by

centrifugation at 33,000 × *g* for 30 min. The samples were analyzed by SDS-PAGE and immunoblotting.

Coimmunoprecipitation from Rat Brain Extract

Rat brain extracts were prepared as described previously (Qualmann *et al*., 2004) and precleared by incubation with protein A agarose (Santa Cruz Biotechnology, Santa Cruz, CA) in 5% bovine serum albumin (BSA) in phosphate-buffered saline (PBS). Equal amounts of affinity-purified guinea pig anti-syndapin I antibodies or unrelated guinea pig immunoglobulins G (IgG) were immobilized onto protein A agarose in 5% BSA in PBS. After several washes with immunoprecipitation (IP) buffer (10 mM HEPES, 1 mM EGTA, 0.1 mM $MgCl_2$, 50 mM NaCl, 1% Triton X-100, pH 7.4), 1 mg of protein of rat brain extract was added. Beads were incubated for 3 h at 4°C, washed with IP buffer, and eluted with SDS sample buffer. Eluates and supernatants were separated on SDS-PAGE and analyzed by immunoblotting.

Preparation of Cell Extracts and Coimmunoprecipitation

For immunoprecipitations of epitope-tagged proteins, HEK293 cells were transiently cotransfected with different GFP- and FLAG-tagged constructs, grown for additional 40 h, harvested, and lysed in IP buffer containing 100 mM NaCl. Insoluble material was removed by centrifugation.

Anti-FLAG antibodies or unrelated mouse IgG (Santa Cruz Biotechnology) were coupled to protein G-Sepharose beads (Amersham Biosciences) at 4°C for 5 h. In some experiments, antibodies were subsequently covalently linked to beads by dimethyl-pimelimidate-dihydrochloride (Fluka Chemical, Ronkonkoma, NY) for 45 min at room temperature (Schneider *et al*., 1982), and HEK293 cell lysates were preincubated at room temperature for 10 min with AMP, ADPβS, ATPγS, or ATP (all from Sigma) and $MgCl_2$ (final concentration each 5 mM). Lysates were incubated with the antibody-coated beads overnight at 4°C. The beads were washed with IP buffer, and eluted immunoprecipitates were subjected to immunoblot analysis.

Yeast Two-Hybrid Analyses

Y2H-screenings were performed using the GAL4-based Matchmaker yeast two-hybrid system 3 (BD Biosciences Clontech) with full-length syndapin I as a bait. Both a rat brain cDNA library and a pretransformed mouse brain library (BD Biosciences Clontech) were screened. Prey plasmids were isolated, retransformed into yeast, and mated with yeast strains transformed with BD-syndapin I, BD-syndapin I ΔSH3, and with the pGBTK7 vector encoding for the BD domain alone. The diploids were subsequently assayed for the activation of reporter genes, as described in Kessels and Qualmann (2002).

Cell Culture and Immunofluorescence Microscopy

HEK293, HeLa, and COS-7 cells were maintained in DMEM containing 10% fetal bovine serum. Primary hippocampal cultures were prepared and grown as described previously (Kessels *et al*., 2001; Qualmann *et al*., 2004).

Primary neurons 15 days in vitro (DIV) were transfected using Lipofectamine 2000 (Invitrogen). Twenty-four hours after transfection, the cells were processed for immunofluorescence as described previously (Qualmann *et al*., 2004). For the evaluation of the specificity and affinity of the guinea pig anti-syndapin I antibodies, COS-7 cells were transiently transfected using the FuGENE reagent (Roche Diagnostics). For mitochondrial targeting experiments, HeLa cells were transfected with Polyfect reagent (QIAGEN, Valencia, CA).

Cells were fixed and processed for immunofluorescence according to Kessels *et al*. (2001). For mitochondrial staining, cells were incubated with MitoTracker Red CMXRos (Molecular Probes) as described previously (Kessels and Qualmann, 2002). Images were recorded digitally using a Leica TCS SP2 AOBS confocal microscope or a Leica DMRD fluorescence microscope and a Zeiss Axioplan 2 microscope both equipped with a charge-coupled device camera 2.1.1 from Diagnostic Instruments (Sterling Heights, MI) and processed in MetaVue and Adobe Photoshop.

Transferrin Internalization Assay

COS-7 cells were subjected to transferrin uptake assays 48 h after transfection as described previously (Qualmann and Kelly, 2000; Kessels and Qualmann, 2002). COS-7 cells treated with BioPorter according to the manufacturer's instructions (Gene Therapy Systems, San Diego, CA) to introduce immunoreagents were subjected to endocytosis assays 5 h after start of treatment. To be able to see putative dose responses, cells were split in three categories differing in the extent of uptake of immunoreagent by the BioPorter method as described by Kessels and Qualmann (2002). The categories can easily be distinguished as follows: weak (gray values as measured in MetaVue 60–119), medium (gray values 120–230), and strong uptake (>90% of cytosol area in saturation, i.e., gray value 255) of the respective immunoreagent. The gray value average for coverslip background was 53. All images were taken at an exposure time of 1000 ms. The percentages of transfected cells showing no detectable uptake of transferrin, significantly reduced transferrin signals, and normal levels of internalized transferrin and standard deviations were calculated by scoring and counting cells in independent experiments as described previously (Qualmann and Kelly, 2000; Kessels *et al*., 2001; Kessels and Qualmann, 2002). The categories used to evaluate endocytosis can be classified as follows: block, no endosomal structures labeled by transferrin are observable at 1000-ms exposure time; reduced, endosomal signal observable but ≤70% intensity of untransfected cells average. This objectivity of our category definitions allows several independent investigators to work in parallel.

Transferrin Recycling Assay

HeLa cells were transfected using Polyfect transfection reagent (QIAGEN) for 24 h. After a 30-min starvation in DMEM containing 20 mM HEPES and 0.2% BSA, pH 7.5, cells were pulsed with 20 μg/ml transferrin-Alexa Fluor 488 or -Alexa Fluor 568 (Molecular Probes) for 10 min at 37°C. Cells were washed twice with ice-cold PBS (containing 0.5 mM $CaCl_2$ and 0.5 mM $MgCl_2$) and labeled transferrin was chased for 20 min at 37°C in DMEM with 10% fetal calf serum, 2 mM glutamine, and 1 mg/ml unlabeled holo-transferrin (Sigma). The cells were washed with $CaCl_2$- and $MgCl_2$-containing PBS and subsequently fixed and processed as described above. All transfected cells on several coverslips were identified by GFP fluorescence or by immunolabeling and scored for remaining transferrin fluorescence. Only cells with a readily detectable transferrin signal were considered positive for transferrin and counted. This corresponded to maximal gray values for endosomal areas (of 5 pixels in diameter) of <40%, as measured via the information palette of Adobe Photoshop. In most cases, endosomal signal intensity maxima reached values close to 0%, which look white (saturation of signal) for the eye (exposure times 2000 ms for transferrin-Alexa Fluor 568 and 5000 ms for transferrin-Alexa Fluor 488). This stringent definition of recycling defects led to a value of ~50% of recycling-inhibited cells upon overexpression of the mRme/EHD1 G429R mutant shown to introduce a prominent block in recycling (Lin *et al*., 2001) and to 20–25% of affected cells in control experiments of different kinds. The objectivity of our category settings allowed us to perform the scoring of the cells by as many as three different investigators. Their results were averaged and subjected to statistical significance calculations using Fisher's protected least significant difference (PLSD) and Dunnett's tests (StatView program; SAS Institute, Cary, NC).

RESULTS

Identification of EHD Proteins as Binding Partners for Syndapin I

Syndapin proteins are involved in vesicle formation processes and in modulation of the actin cytoskeleton, because they interact with the GTPase dynamin and with the Arp2/3 complex activator N-WASP through their C-terminal SH3 domain (Kessels and Qualmann, 2004). Because syndapins contain several additional protein–protein interaction modules such as predicted N-terminal coiled coil domains, NPF motifs, and a variety of consensus sites for different kinases, syndapins may act as multidomain scaffolding proteins integrating several different cellular functions. The three syndapin isoforms expressed in mammals show a highly conserved domain structure (Figure 1A). At the amino acid level, conservation between the isoforms is also very high. This is especially true for the C-terminal SH3 domains (Kessels and Qualmann, 2004). An exception is the NPF motif-containing regions N-terminal of the SH3 domains. They differ both in amino acid composition and in number of the NPF motifs. NPF motifs are absent in syndapin III (Figure 1A).

In yeast two-hybrid screens with a syndapin I full-length bait (Figure 1A) using different brain cDNA libraries, we obtained cDNA clones that encoded fragments of EHD3, a member of the EHD protein family implicated in endocytic recycling. The fragments encompassed part of the putative coiled coil domain and the C-terminal EH domain (Figure 1B). Analyses of reporter gene activities in yeast strains coexpressing the syndapin I bait yielded robust growth on drop-out plates of different stringency (Figure 1C) and clear positive signals in β-galactosidase assays (Figure 1D). The interaction was independent of the syndapin SH3 domain (Figure 1, C and D). We verified the interaction by affinity purification experiments. Both a C-terminal fragment and full-length EHD3 fused to GST specifically precipitated endogenous syndapin I from rat brain cytosol (Figure 1E).

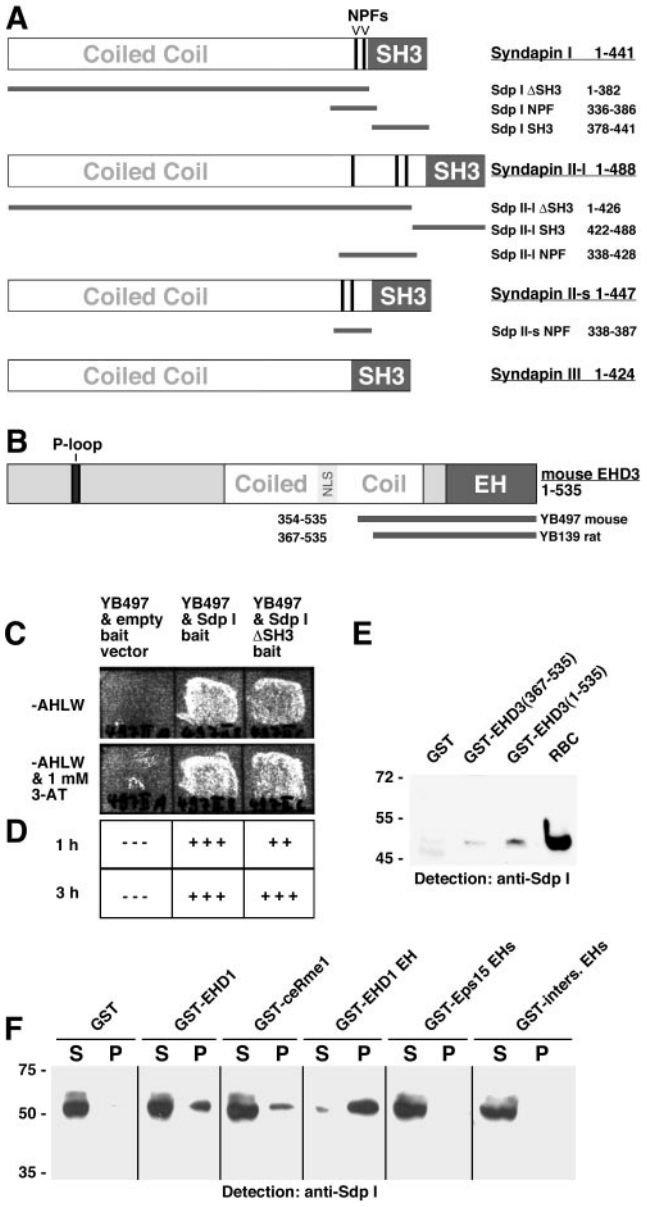

Figure 1. Syndapin I interacts specifically with EH domain-containing proteins of the EHD protein family. (A) Schematic representation of the syndapin isoforms and splice variants syndapin I, II-s, II-l, and III as well as of the different syndapin fragments used throughout this study (solid bars). (B) Schematic representation of the EH domain-containing protein EHD 3 and of two independent clones encoding for the C terminus isolated by Y2H screening with full-length syndapin I as a bait. (C and D) Activation of reporter genes assayed via growth on quadruple drop-out plates (C) and via β-galactosidase activity (D). (E) Affinity purifications of endogenous syndapin I from rat brain cytosol (RBC) with immobilized GST-fusion proteins of an EHD3 fragment and of full-length EHD3, verifying the Y2H results. (F) Affinity purifications of endogenous syndapin I from rat brain extracts with immobilized GST-fusion proteins of different EH domain-containing proteins reveal that syndapin I associates with EHD proteins but not with the EH domains of intersectin or Eps15. Equal amounts of fusion proteins and rat brain cytosol (1 mg) were used. Twenty micrograms of starting material was loaded for comparison. P, precipitates; S, supernatants.

EH domains are present in a variety of proteins involved in membrane trafficking processes. Thus, we asked whether the syndapin interaction is restricted to EHD3, or whether it also occurs with multiple members of the EHD protein family or whether the interaction is promiscuous for many EH domain-containing proteins (Figure 1F). Syndapin I was successfully coprecipitated from rat brain extracts by immobilized GST-fusion proteins of full-length mouse Rme-1/EHD1 and of the only member of the EHD protein family in *C. elegans*, ceRme-1 (Figure 1F). The EH domain of mouse Rme-1/EHD1 alone was sufficient for the interaction. Interestingly, the EH domains of both Eps15 and intersectin failed to interact with syndapin I, although all three EH domains of Eps15 and the two EH domains of intersectin were used (Figure 1F). Syndapin I thus exhibits specificity for EH domains found in members of the EHD protein family.

EHD Proteins Are Differential Binding Partners of the Syndapin Family

We next evaluated whether the identified interaction with EHD proteins is a specialty of syndapin I. Coprecipitation analyses demonstrated that syndapin I, syndapin II-s, and syndapin II-l but not syndapin III interact with endogenous EHD proteins. The strongest interaction was observed with syndapin II-l (Figure 2, A and B).

The molecular properties underlying these differential syndapin interactions were revealed in coprecipitation experiments with different immobilized GST fusion proteins of syndapin I (Figure 2, C and D) and syndapin II (Figure 2, E and F). EHD proteins were precipitated from rat brain extracts by GST-fusion proteins of full-length syndapin I and of syndapin I ΔSH3, but not by the SH3 domain alone (Figure 2D). The interaction was further narrowed down to the non-SH3 part encompassing the NPF motifs (Sdp I-NPF) (Figure 2, C and D). Similar results were obtained with the more ubiquitously expressed syndapin II isoform. The interaction was independent of the syndapin II SH3 domain. The NPF regions alone of both syndapin II-s and syndapin II-l were sufficient to precipitate EHD proteins (Figure 2, E and F). Similar data were obtained using GFP-mRme-1/EHD1 overexpressed in HEK293 cells (our unpublished data). The sequence conservation of the region of syndapin proteins encompassing the NPF motifs is relatively high between syndapin I and II (Figure 2G). Interestingly, the additional amino acid insert present in the syndapin II-l splice variant contains a third NPF motif. In contrast, syndapin III lacks NPFs (Figures 1A and 2G).

The observed differential associations of syndapins (Figure 2B) prompted us to examine putative specificities for different EHD proteins as well. We therefore cloned all four mouse EHD isoforms, which are highly conserved and despite the phylogenetic distance also show a high homology with the *C. elegans* ortholog (Figure 2H). Immobilized GST-fusion proteins of syndapin I (Figure 2J), syndapin II-s (Figure 2K), and syndapin II-l (Figure 2L), but not GST alone (our unpublished data) efficiently precipitated GFP-mRme-1/EHD1, GFP-EHD3, and GFP-EHD4 from HEK293 cell extracts. The amount of GFP-EHD2 within the precipitates of all three syndapins was low (Figures 2, J–L). Thus, syndapins strongly bound only to three of the four EHD proteins, the relatively widely distributed mRme-1/EHD1, which our phylogenetic analyses suggest to be closest to the EHD ancestor (our unpublished data), EHD3, an isoform highly expressed in brain but also occurring in other tissues and the heart-enriched EHD4 (Pohl *et al*., 2000; Galperin *et*

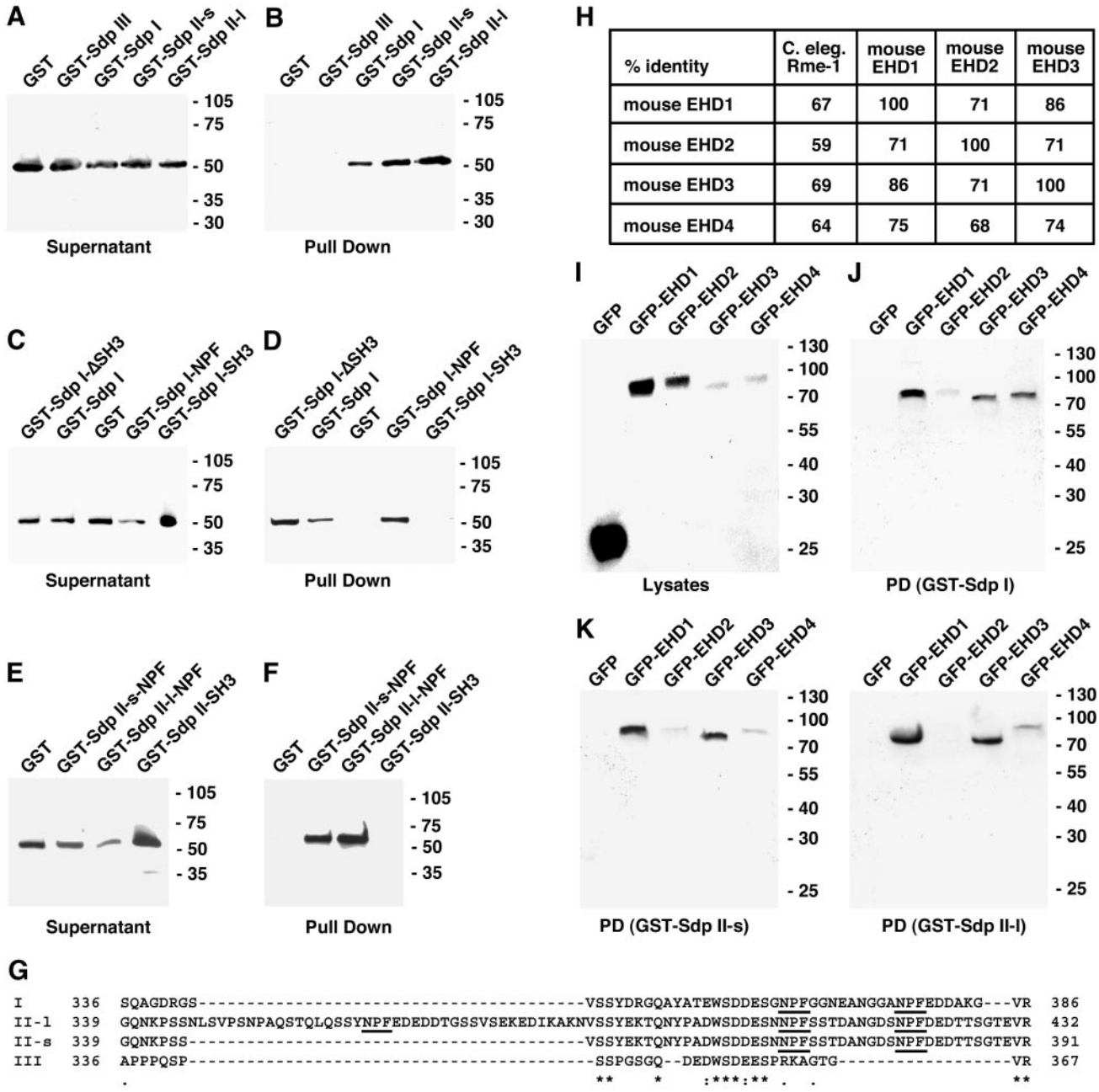

Figure 2. The interaction with EHD proteins is mediated by the NPF motif-encompassing region present in syndapin I and II. (A–F) Precipitates and supernatants from coprecipitation experiments with immobilized GST-fusion proteins of syndapins incubated with rat brain extracts (1 mg of protein each) were analyzed by immunoblotting with anti-EHD antibodies. (A and B) GST fusion proteins of syndapin I and of both syndapin II splice variants (Sdp II-s and Sdp II-l), but not of syndapin III or GST alone, efficiently coprecipitated endogenous EHD proteins. (C–F) Experiments with immobilized GST-fusion proteins of syndapin I (C and D) and syndapin II (E and F) reveal that the interaction of both syndapin I and II is mediated by the NPF motif-containing region (Sdp-NPF). (G) Alignment of the amino acid sequences of rat syndapin I (gi4324451, aa 336–386), rat syndapin II-s (gi6651165, aa 339–391), rat syndapin II-l (gi6651162, aa 339–432), and rat syndapin III (gi57471977, aa 336–367) by ClustalW (http://www.ebi.ac.uk/clustalW/). (H) Amino acid sequence identity between all four murine EHD family members as well as *C. elegans* Rme-1. (I–L) Coprecipitation analyses with extracts from HEK293 cells expressing GFP-fusion proteins of all four mouse full-length EHD proteins or GFP alone (I) and immobilized GST-fusion proteins of full-length syndapins. Whereas immobilized GST did not precipitate any GFP-fusion proteins (our unpublished data), the coprecipitates obtained with immobilized syndapin I (J), syndapin II-s (K), and syndapin II-l (L) revealed strong associations of all these syndapin variants with all EHD proteins except EHD2, as analyzed by anti-GFP immunoblotting.

al., 2002). EHD1, 3, and 4 show a good expression overlap with the syndapin isoforms I and II and their splice variants. In contrast, the isoform not effectively bound by syndapins, EHD2, is highly expressed in muscle tissues (Pohl *et al*., 2000) where expression of syndapin I and II is very low and not detectable, respectively (Qualmann and Kelly, 2000).

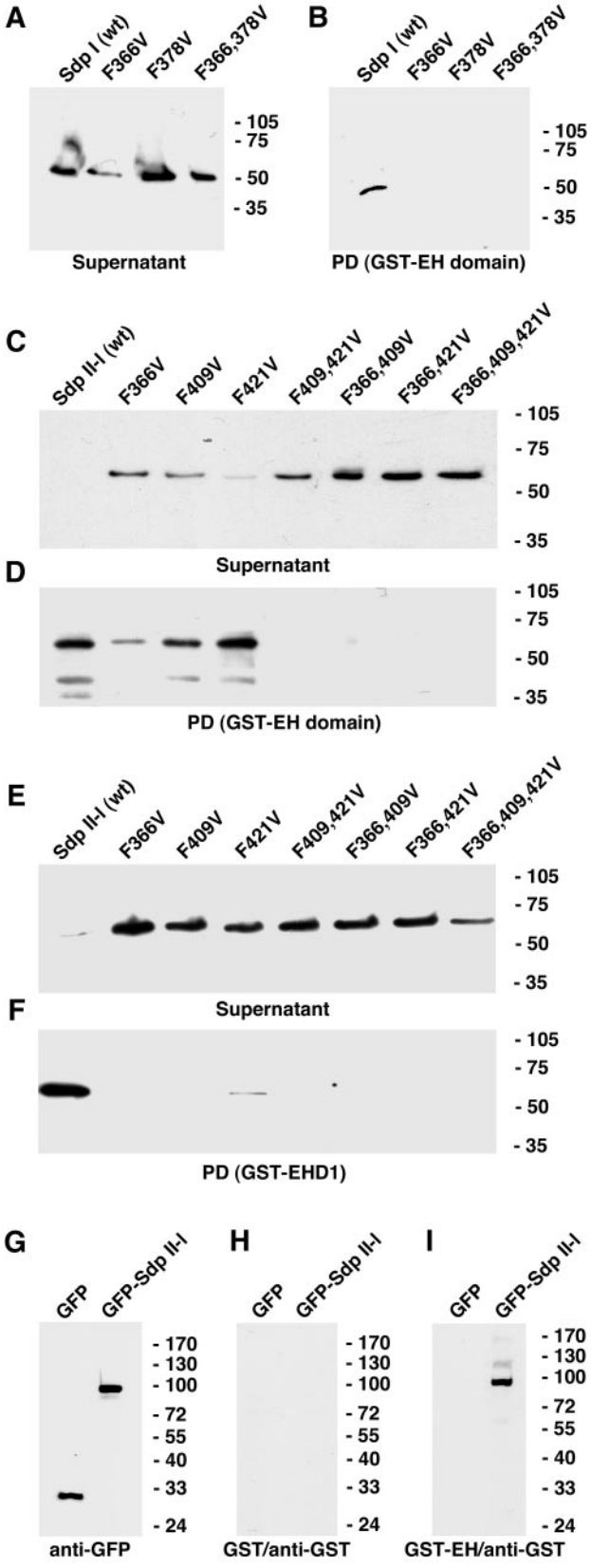

Figure 3.

Syndapin NPF Motifs Are Crucial for the Association with the EH Domain of EHD Proteins and the Interaction Is Direct

Our in vitro analyses clearly demonstrated that regions of syndapins that contain NPF motifs are sufficient for the interaction with EHD proteins (Figure 2). To directly prove that the NPF motifs are crucial and to identify which of the several NPF motifs is responsible for the interaction, we mutated all NPF motifs in syndapin I and II individually and in combination to asparagine proline valine (NPV) and expressed all constructs in HEK293 cells. Immobilized GST-fusion protein of the EH domain of mRme-1/EHD1 only precipitated wild-type syndapin I. Mutating the two NPFs of syndapin I individually or in combination abolished the interaction (Figure 3, A and B), indicating that the NPF motifs are crucial for the interaction with mRme-1/EHD1 and that both NPFs are required in combination.

For syndapin II-l, we observed that mutating one of the three NPFs still permitted some association with the EH domain of mRme-1/EHD1. The F421V mutation showed the least and the F366V mutation showed the strongest negative effect (Figure 3, C and D). Mutating two NPF motifs abolished the interaction with the mRme-1/EHD1 EH domain completely irrespective of the combination of mutations. Consistently, the syndapin II-l (F366V, F409V, F421V) triple mutant showed no interaction (Figure 3, C and D).

The presence of at least two syndapin NPF motifs is also important for EH domain binding in the full-length context of EHD. Wild-type syndapin II-l was almost quantitatively precipitated from the cell extracts by full-length mRme-1/EHD1 but binding was almost completely abolished in mutants with a single NPF to NPV amino acid exchange. Only for syndapin II-l F421V some binding to full-length mRme-1/EHD1 was observed (Figure 3, E and F). Thus, the interaction is highly dependent on the presence of multiple NPF motifs within syndapins.

Our analyses of the binding interfaces showed that both NPF motifs and EH domains are required and sufficient for the interaction. Because these motifs are known to interact, this suggested that the interaction between syndapins and EHD proteins may be direct. To prove this, we overlaid lysates from HEK293 cells containing GFP-syndapin II-l or GFP as a control (Figure 3G) with a GST-EH domain probe. In the lane with the overexpressed GFP-syndapin II-l, the GST-EH probe readily detected a 90-kDa band that was absent in the GFP control lane (Figure 3I) and corresponded well with the band of GFP-syndapin II-l obtained by anti-GFP immunoblotting (Figure 3G). Additionally, several weaker bands were revealed by the GST-EH domain at ~60, 120, and 170 kDa in the lane with GFP-syndapin II-l. Because these were absent from the HEK293 cell lysate containing GFP alone and were not detected by anti-GFP antibodies,

Figure 3. The interaction between syndapins and EHD proteins is direct and depends on syndapin NPF motifs. (A–F) Immunoblot analyses of coprecipitations of FLAG-tagged wild-type and mutant syndapin I (A and B) and syndapin II-l (C–F) proteins overexpressed in HEK293 cells with immobilized GST-fusion proteins of the EH domain of EHD1 (A–D) and of full-length EHD1 (E and F). The coprecipitated material (B, D, and F) and the supernatants (A, C, and E) were analyzed by immunoblotting with anti-FLAG antibodies. (G–I) Blot overlay analysis of extracts from HEK293 cells overexpressing GFP and GFP-Sdp II-l. Overexpressed proteins were visualized by anti-GFP immunoblotting (G), with a GST-fusion protein of the EH domain of EHD1 (I) and GST (negative control) (H) as probes.

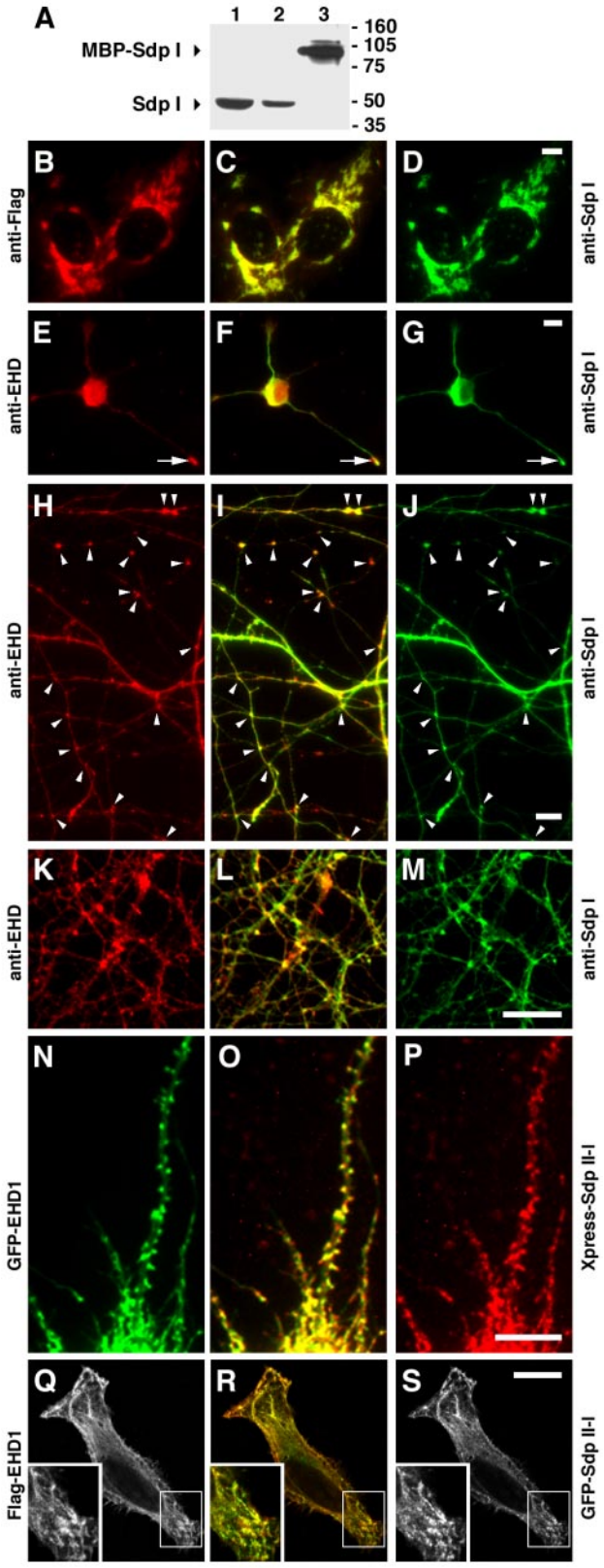

Figure 4.

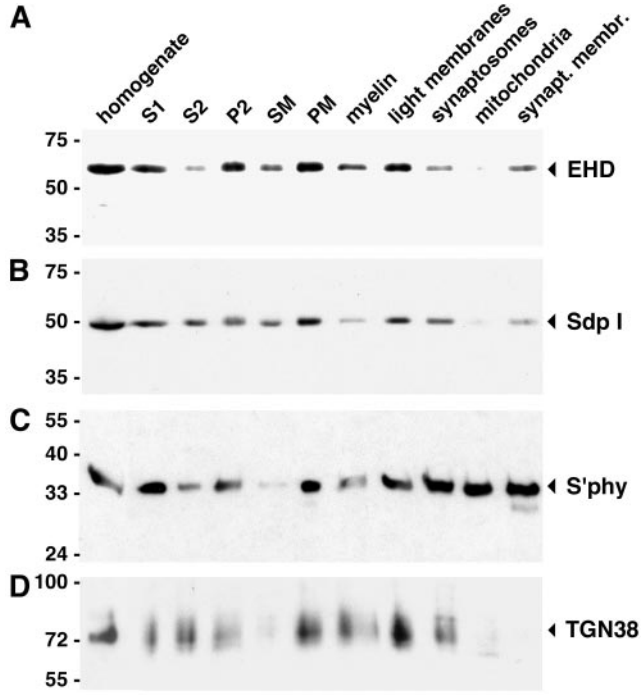

Figure 5. EHD and syndapin proteins are codistributed in rat brain fractions. Western blots of rat brain homogenate and indicated subcellular fractions probed with antibodies against EHD proteins (A), syndapin I (B), the synaptic vesicle marker synaptophysin (C), and the TGN marker protein TGN38 (D). S1, 1000 × *g* supernatant 1; S2, 12,000 × *g* supernatant 2; P2, 12,000 × *g* pellet 2 (crude membrane fraction). Myelin, light membranes, synaptosomes, and the fraction containing heavy membranes and mitochondria (mitochondria) were obtained by sucrose step gradient separation of P2. SM, 100,000 × *g* microsomal supernatant; PM, 100,000 × *g* microsomal pellet.

they cannot represent endogenous proteins or GFP fusion proteins, but instead are likely to represent syndapin II-l proteins released from GFP by proteolysis. The molecular masses that we observed fit with syndapin II-l monomers

Figure 4. Syndapins and EHD proteins colocalize in neuronal and nonneuronal cells. (A) The new guinea pig anti-syndapin I antibodies specifically recognize syndapin I on Western blots of 25 μg (lane 1), 5 μg (lane 2) of rat brain extracts and 50 ng of MBP-syndapin I ΔSH3 (lane 3). (B–D) The affinity-purified anti-syndapin I antibodies (D) recognize FLAG-tagged mito-syndapin I expressed in COS-7 cells with the same specificity as monoclonal anti-FLAG antibodies (B), as seen by the complete overlap of the stainings in the merge (C). (E–M) Primary hippocampal neurons 2 DIV (E–G) and 24 DIV (H–M) were immunostained with anti-syndapin I antibodies (G, J, and M) and anti-EHD antibodies (E, H, and K). Colocalization is in yellow in merged images (F, I, and L). Examples of growth cones (E–G, arrow) and of sites within the periphery of the neuronal network that may represent synaptic contacts and also display an accumulation for both syndapin I and EHD proteins are marked (H—J, arrowheads). (N–O) GFP-EHD1 (N) and Xpress-syndapin II-l (P) expressed in primary hippocampal neurons also show a high degree of spatial overlap (O). (Q–S) FLAG-tagged EHD1 (Q, red in merge) and GFP-syndapin II-l (S, green in merge) coexpressed in HeLa cells exhibit a similarly high degree of colocalization, as observed by confocal microscopy. Insets represent magnifications of areas boxed. Bars, 10 μm.

(60 kDa), syndapin II-l dimers (120 kDa), and syndapin II-l trimers (~170 kDa). In contrast, GST alone used as a control probe did not yield any signal (Figure 3H). These blot overlay studies formally demonstrate a specific and direct interaction of syndapins with the EH domain of EHD proteins.

Syndapins and EHD Proteins Are Codistributed in Neuronal and Nonneuronal Cells

To address in which cells and subcellular compartments the interaction between syndapins and EHD proteins might be of physiological importance, we subsequently performed colocalization studies (Figure 4). For this purpose, we raised new anti-syndapin I antibodies in guinea pigs. In immunoblot analyses, they recognized a single band of the expected size for syndapin I (~50 kDa) in brain extracts (Figure 4A, lanes 1 and 2) and also detected recombinant MBP-syndapin I ΔSH3 (lane 3) with high-affinity. In immunofluorescence examinations, they detected FLAG-tagged mito-syndapin I expressed in COS-7 cells (Figure 4D) as specifically and efficiently as anti-FLAG antibodies applied in parallel (Figure 4B). In primary hippocampal neurons kept in culture for 2 days, syndapin I was localized to the soma and to neurites and displayed accumulations at actin-rich growth cones (Figure 4G, arrow). The distribution of anti-EHD immunosignal was very similar (Figure 4E) and overlapped well with that of syndapin I (Figure 4F).

As described previously (Qualmann *et al*., 1999), in mature neurons, syndapin I adopts a more punctate synaptic distribution in addition to the neuritic localization, as seen best in low-density cultures at lower magnification (Figure 4J). Anti-EHD immunosignals (Figure 4H) also were obtained throughout neurites and showed, in part, strong accumulations at puncta that were always also immunopositive for syndapin (Figure 4J, arrowheads). These were often at sites where neurites contacted one another (Figure 4, H–J). At higher magnification, we observed a very exact spatial overlap of anti-syndapin I and anti-EHD immunosignals at sites that are likely to represent synapses (Figure 4, K–M).

Analyses of endogenous syndapin II in cultured neurons were precluded by low syndapin II expression in brain (Qualmann and Kelly, 2000). We thus slightly overexpressed syndapin II-l (Figure 4P) together with GFP-mRme-1/EHD1 (Figure 4N) in primary hippocampal neurons. The merge of both images demonstrates the observed very high spatial overlap of both proteins in dot-like structures of a single transfected cell that often protrude from the neurites and may represent synaptic sites (Figure 4O). Both proteins also colocalized in cell somata (our unpublished data). Because both proteins were coexpressed in single, isolated cells within the neuronal cultures and showed a colocalization within these cells, it can be firmly concluded that the two proteins coexist in puncta representing the same synaptic compartment, i.e., it can be excluded that the two proteins are separated by the synaptic cleft between a pre- and a postsynaptic neuron. Because these puncta were observed in several neurites originating from the cell, we can furthermore conclude that syndapin and EHD1 coexist in the dendritic compartment and that the puncta thus represent postsynapses. A putative presynaptic localization of EHD1 remains to be confirmed by immunoelectron microscopy.

In nonneuronal cells, such as HeLa cells, FLAG-mRme-1/EHD1 (Figure 4Q) and GFP-syndapin II-l (Figure 4S) also showed a strong spatial overlap, especially at structures that looked tubular and vesicular (Figure 4R).

Our immunofluorescence data suggest that syndapins and EHD proteins both localize to several cellular membrane compartments. Biochemical subcellular fractionation analyses and preparations of different membrane and synaptic compartments from brain homogenates indeed revealed that EHD proteins are especially abundant in membrane-associated fractions but low in fractions that contain more soluble proteins (Figure 5A). Strong anti-EHD immunosignals were seen in the crude membrane fraction P2, whereas in the corresponding supernatant S2, the signal was very low. The fractionation of S2 showed that this material mostly reflected microsomal pellet material. When the crude membrane fraction P2 was analyzed further, it became obvious that EHD immunoreactivity was enriched strongest in the light membrane-enriched fraction and was especially low in the fraction containing mitochondria and heavy membranes. Our preparations of synaptosomes and synaptic membranes were positive for anti-EHD immunosignals (Figure 5A).

Syndapin I showed a distribution very similar to that of EHD proteins (Figure 5B). Both the material obtained in S2 and in the crude membrane fraction P2 fractionated further in a manner identical to that of EHD proteins. As with the EHD immunoreactivity, syndapin I accumulated in the microsomal pellet rather than in the high speed cytosol. Also similar to the anti-EHD pattern, syndapin I was readily detected in light membranes and synaptosomes but absent from the heavy membrane- and mitochondria-containing fraction (Figure 5B, mitochondria). Together with EHD, syndapin I was detectable in the preparation of synaptic membranes (Figure 5B). The anti-syndapin II immunosignal was extremely weak (our unpublished data). The low immunosignals obtained are in line with the fact that the expression level of the more ubiquitously expressed syndapin II isoform is low in brain (Qualmann and Kelly, 2000).

The similarity of the subcellular fractionation pattern of EHD proteins and syndapin I is highlighted best by comparison with other proteins, such as the synaptic vesicle protein synaptophysin (Figure 5C) and the trans-*Golgi* marker TGN38 (Figure 5D). Synaptophysin, in contrast to syndapin and EHD, cannot be detected in the SM fraction but for example strongly accumulates in synaptosomes and in the preparation of synaptic membranes (Figure 5C). TGN38 shows a very different pattern. Very little TGN38 was found in the synaptosome fraction. Also, TGN38 is abundant in S2 and relatively scarce in P2. No TGN38 immunoreactivity was detected in the synaptic membrane preparation (Figure 5D).

Syndapin I and Syndapin II-l Interact with EHD Proteins In Vivo

To address whether syndapins and EHD proteins interact in vivo, we coexpressed GFP-syndapin II-l (Figure 6, A–D) or GFP-syndapin I (Figure S2) together with FLAG-tagged mRme-1/EHD1 in HEK293 cells and subjected the lysates to coimmunoprecipitations. In both experimental series, FLAG-mRme-1/EHD1 was effectively and specifically immunoprecipitated by anti-FLAG antibodies (Figures 6B and S2), whereas in the control experiments FLAG-mRme-1/EHD1 remained in the supernatants (Figures 6A and S2). GFP-syndapin II-l was specifically coimmunoprecipitated with FLAG-mRme-1/EHD1 by anti-FLAG antibodies but not by the control IgGs (Figure 6D). GFP was not coimmunoprecipitated, demonstrating that indeed the syndapin part interacts with mRme-1/EHD1 (our unpublished data; compare Figure 10). Consistent with our in vitro data, GFP-syndapin I was also specifically coimmunoprecipitated with FLAG-mRme-1/EHD1 (Figure S2).

We also were able to specifically immunoprecipitate endogenous syndapin I from rat brain extracts with our guinea

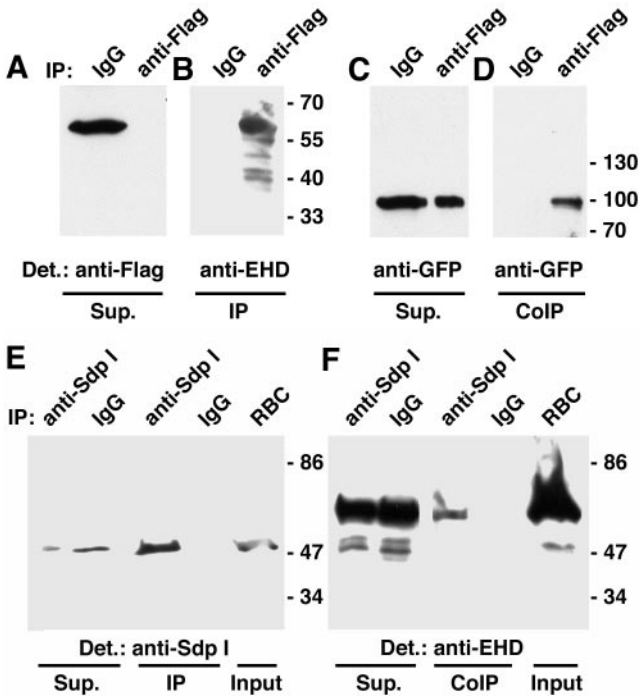

Figure 6. Syndapin I and II-l coimmunoprecipitate with EHD proteins. (A–D) Coimmunoprecipitation of GFP-syndapin II-l with FLAG-EHD1 coexpressed in HEK293 cells. Immunoblot analyses of immunoprecipitates (B and D) and supernatants (A and C). (E and F) Immunoblot analyses of supernatant, immunoprecipitated material and of the rat brain extract used for coimmunoprecipitations of endogenous EHD proteins along with endogenous syndapin I, which was immunoprecipitated by anti-syndapin I antibodies.

pig anti-syndapin I antibodies (Figure 6E). EHD proteins were specifically coimmunoprecipitated (Figure 6F), showing that syndapin/EHD protein complexes exist in vivo.

The Strength of the EH Domain-mediated Interaction of mRme-1/EHD1 with Syndapin II Is Sufficient for a Recruitment of Syndapin to Intracellular Membranes In Vivo

Because EHD proteins were found to be predominantly membrane-associated (Figure 5), a property that is consistent with its subcellular localization (Figure 4) and proposed function (Lin *et al*., 2001; Caplan *et al*., 2002; Naslavsky *et al*., 2004), we next assayed whether EHD proteins would be able to recruit cytosolic syndapins to intracellular membranes. We constructed a mitochondrially targeted EH domain of mRme-1/EHD1 fused to GFP. This fusion protein was effectively targeted to the outer mitochondrial membranes of HeLa cells (Figure 7A), as shown by Mito-Tracker staining (Figure 7C). When full-length syndapin II-l was coexpressed, it adopted a mitochondrial localization pattern (Figure 7F) overlapping exactly with mito-GFP-EH–coated mitochondrial membranes (Figure 7D). Also syndapin II-l ΔSH3 was very effectively recruited by mitochondrial membrane-associated EH domains of mRme-1/EHD1 (Figure 7, J–L). In both cases, mitochondria decorated with the EH domain became clustered, whereas this was not observed in cells overexpressing the mitochondrially targeted EH domain of mRme-1/EHD1 alone (Figure 7A). The successful in vivo reconstitution of the protein interaction at cellular membranes was based on a specific interaction of the EH domain of mRme-1/EHD1 with syndapin II-l. In control cells expressing only mito-GFP (Figure 7G), no such recruitment of syndapin II-l (Figure 7I) or syndapin II-l ΔSH3 (our unpublished data) to mitochondria was observed, but both syndapin fusion proteins remained relatively evenly distributed within the cytosol. Consistent with our in vitro studies, these findings demonstrate that the NPF-containing N-terminal part of syndapin II-l is sufficient for the interaction in vivo and that the SH3 domain is not required. These experiments furthermore highlight the strength of the EHD/syndapin II interaction at membranes in vivo.

Acute Interference with Syndapin Protein Complexes by Introduction of Anti-Syndapin Antibodies Inhibits Endocytosis

The recycling function of mRme-1/EHD1 was first revealed by dominant negative studies (Lin *et al*., 2001) that were later corroborated by a generalized reduction in mRme1/EHD1 protein levels via RNA interference (RNAi) (Naslavsky *et al*., 2004). Because we found that syndapins and EHD proteins associate tightly in vivo, we sought to determine whether syndapins function with EHD proteins in receptor recycling. One method we applied to this problem was a general interference with the presence and/or function of syndapin complexes by the introduction of antibodies. The introduction of anti-syndapin antibodies raised against the C terminus of syndapin I, including the SH3 domain region into COS-7 cells, however, resulted in a strong dose-dependent interference with the uptake of transferrin (Figure 8), precluding analysis of transferrin recycling. At medium levels of immunoreagent uptake, about one-half of the cells were clearly affected. At higher levels, ~50% of the cells showed a complete block in transferrin uptake. The effects were specific for the anti-syndapin antibodies because neither the uptake reagent (BioPorter) alone nor fluorescently labeled control IgGs caused any significant effects. Also the preimmune antibodies corresponding to the inhibiting anti-syndapin immunoreagent did not result in any inhibitory effects (Figure 8). These results indicate that syndapins are important for endocytic vesicle formation and that acute interferences with syndapin functions by the introduction of anti-syndapin antibodies cannot be compensated for by affected cells.

Transferrin Receptor Recycling Is Impaired by Overexpression of Syndapin II-l NPF Motifs, the Binding Interface for EHD Proteins

The above-mentioned experiments show that interfering with syndapin functions in total introduces a block early in the endocytic pathway, at the step of vesicle formation at the plasma membrane and thus precluded to address syndapin functions in processes further downstream of endocytic vesicle formation. We hypothesized that mechanistic details of a potential recycling function for syndapin might be revealed by specifically disrupting interactions of certain domains of syndapins rather than by interfering with the protein in toto. A prerequisite is that unlike the SH3 domain (Qualmann and Kelly, 2000; Kessels and Qualmann, 2002), these domains must not be involved in vesicle formation at the plasma membrane. Therefore, we turned to dominant-negative experiments to interfere specifically with the assembly of syndapin/EHD complexes. If such a particular syndapin interaction is required for recycling but not for internalization, then overexpression of the domains from either syndapins or an EHD protein mediating that interaction would be expected to inhibit recycling and trap endocytic cargo in the endosomal recycling compartment.

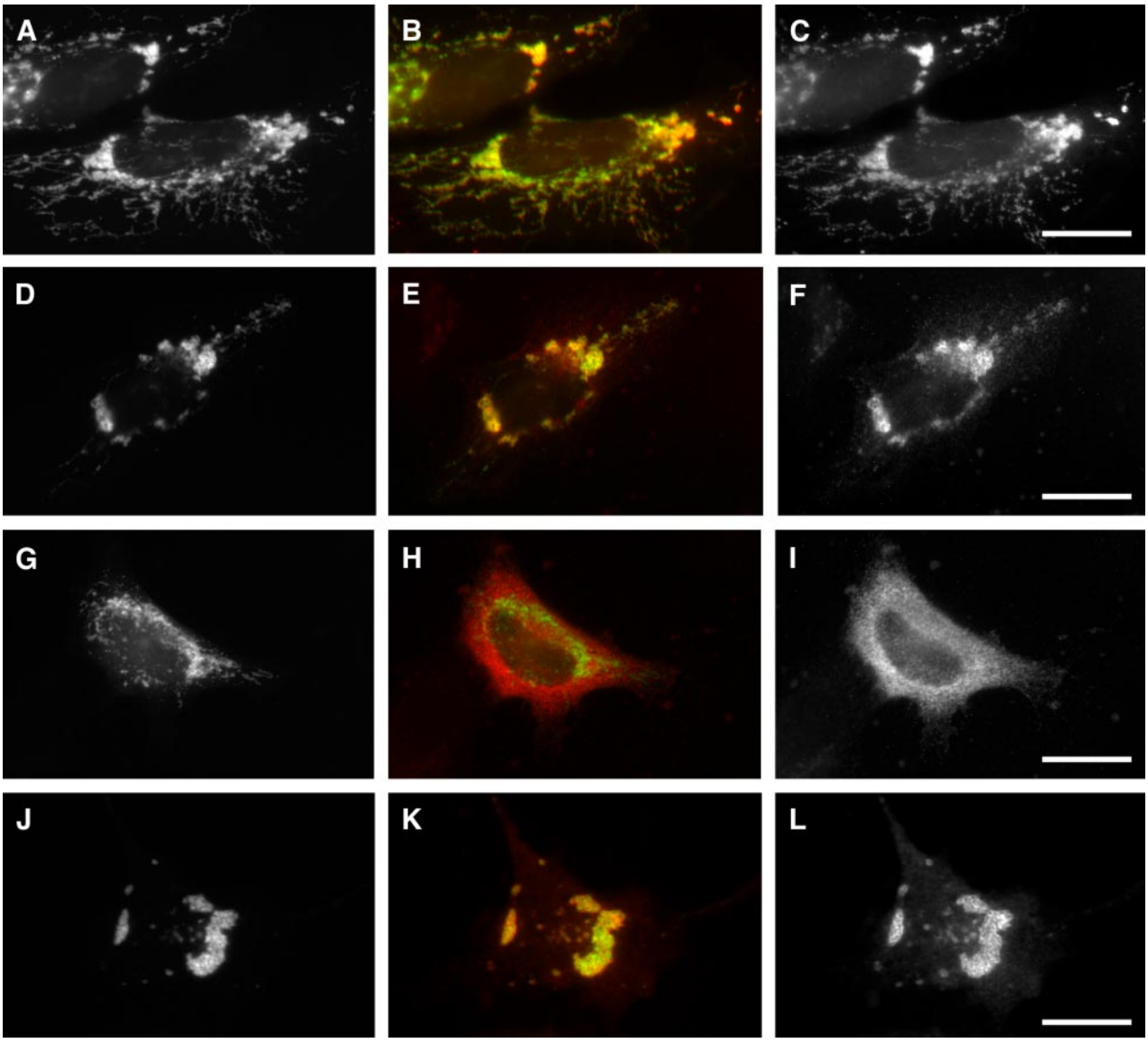

Figure 7. Syndapin II is recruited to mitochondria by a mitochondrially targeted EH domain of EHD1. (A–C) Mito-GFP-EH (A) is efficiently targeted to mitochondria of HeLa cells stained by Mito-Tracker (C). (D–F and J–L) Mitochondrially targeted EH domain (D and J) recruited both coexpressed full-length Xpress-syndapin II-l (F) and Xpress-syndapin II-l ΔSH3 (L). (G–I) In contrast, in cells cotransfected with the mito-GFP vector (G), no such recruitment was observable, but Xpress-syndapin II-l (I) shows diffuse localizations. B, E, H, and K are corresponding merged images. Bars, 20 μm.

To be able to test this hypothesis, we first characterized all such reagents for putative defects prior to the recycling step. As already reported for full-length syndapin II-l (Kessels and Qualmann, 2002), overexpression of the NPF region of syndapin II-l and its corresponding NPF-to-NPV triple mutant did not cause any significant uptake defects (Figure S3). Furthermore, no significant endocytic internalization defects were observed upon overexpression of various mRme-1/EHD1 constructs. Only the G429R mutant showed a modest impairment of transferrin uptake, because only ~70% of the cells showed wild-type internalization (Figure S3).

Thus, we next assayed receptor recycling using methods similar to those described by Lin *et al*. (2001). Untransfected cells preloaded with fluorescently labeled transferrin displayed very low levels of intracellular transferrin after 20 min of chase due to efficient transferrin recycling (see untransfected cells in Figure 9, A–C, and E–G). Only ~20% of the untransfected cells showed a readily detectable endosomal labeling pattern at this time point (Figure 9D). In contrast, overexpression of the syndapin II-l region encompassing the NPF motifs as a GFP-fusion protein led to a massive impairment of transferrin recycling (44% transferrin positive; $p < 0.0001$) visible by the strong increase of fluorescent transferrin that remained within transfected cells after chase (Figure 9A). This value is more than twice as high as in untransfected and GFP-expressing control cells (Figure 9D). Overexpression of the corresponding triple NPF to NPV mutant (GFP-NPF***), which was unable to bind to EHD proteins (Figure 3, C–F), did not lead to recycling defects (Figure 9, B and D), indicating that the syndapin NPF motifs within the NPF motif-containing region of the protein are responsible for the observed block in recycling.

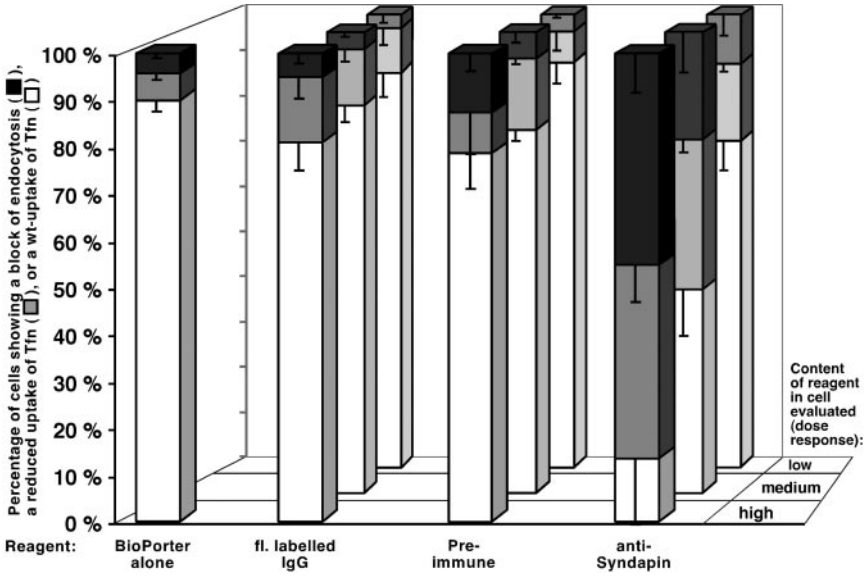

Figure 8. Interference with the function of endogenous syndapin II by introduction of anti-syndapin immunoreagents leads to endocytosis impairments. Quantitation of endocytosis of FITC-transferrin in COS-7 cells incubated with BioPorter to introduce immunoreagents. Percentages of cells blocked (dark), reduced (gray), or wild-type (white) for endocytosis for weak (back row; gray values 60–119), medium (middle row; gray values 120–230), and strong content (front row; >90% of cytosol area in saturation [gray value 255]) of the respective immunoreagent in the cells evaluated. Note that the anti-syndapin immunoreagent #2521 directed against the C terminus of syndapin I, including the SH3 domain led to a dose-dependent impairment (381 cells), whereas BioPorter alone (322 cells) and the two different control immunoreagents (preimmune #2521 [555 cells] and fluorescently labeled IgG [670 cells]) did not.

Because the overexpression phenotypes in endocytic recycling were clearly induced by interfering with EH domain/NPF motif interactions, we next tested whether the NPF-induced effect could be rescued by co-overexpression of mRme-1/EHD1. Examination of the double-transfected cells showed that the NPF-induced phenotype was abrogated (Figure 9C). This indicated that reduced mRme-1/EHD1 activity was responsible for the NPF-induced recycling defect. Quantitation of the data demonstrated that only 28% of the cells displayed transferrin signal (Figure 9D). This value was not significantly different from the values for untransfected cells, GFP-, GFP-NPF***-, or mRme-1/EHD1–overexpressing cells (Figure 9D), as revealed by statistical significance calculations. Compared with overexpression of the construct that contains the NPF region but not the motifs (GFP-NPF***) co-overexpression of mRme-1/EHD1 rescued 81% of the recycling defect caused by overexpression of syndapin NPFs. The efficiency of the rescue was even 113% compared with overexpression of mRme-1/EHD1 alone. This highlights the high potential of full-length mRme-1/EHD1 to rescue the phenotype caused by overexpression of syndapin NPFs and suggests that such EH domain-mediated mRme-1/EHD1 interactions are crucial for receptor trafficking back to the plasma membrane.

Receptor Recycling Is Impaired by EH Domain Overexpression and Can Be Rescued by Syndapin Co-overexpression

Because the specific interference with EH domain functions by overexpression of its syndapin interaction interface led to impairments in receptor recycling (Figure 9, A–D), we next asked whether interfering with NPF/EH domain interactions from the opposite side of the association interface also would inhibit. Indeed, overexpression of a GFP-tagged EH domain inhibited recycling, as shown by the significantly increased transferrin retention in transfected cells (Figure 9E). Quantitation of the dominant-negative effects revealed that the impairment was almost as strong as the effect caused by the syndapin NPF motifs and highly significant. Forty-one percent of all GFP-EH domain-overexpressing cells showed a readily observable endosomal transferrin fluorescence compared with only 22% in GFP controls (Figure 9H).

We subsequently tried to rescue the GFP-EH domain effect by co-overexpression of full-length, i.e., presumably functional, syndapin. We first assayed whether overexpression of syndapin alone would have any negative effects on recycling of transferrin. Both Xpress- and FLAG-tagged syndapin II-l–overexpressing cells showed a transferrin recycling indistinguishable from that of untransfected or GFP-expressing cells (Figure 9, F and H). On double transfection of FLAG-syndapin II-l and mRme-1/EHD1 EH domain (Figure 9G), we observed a normal recycling, indicating a rescue of the EH domain induced phenotype. Only 28% of all double-transfected cells remained positive for fluorescent transferrin compared with 41% in the experiments with the EH domain alone (Figure 9H). Thus, ~66% of the effect caused by overexpression of the EH domain was rescued by coexpression of the mRme-1/EHD1 binding partner syndapin II-l. The values obtained upon our rescue experiments did not significantly differ from control, as revealed by statistical analyses. These data indicate that complexes of syndapins and EHD proteins play an important role in receptor recycling.

EH Domain Interactions with Syndapins Seem to Be Controlled by the Nucleotide-binding Domain of mRme-1/EHD1 In Vitro and In Vivo

Our data show that interfering with NPF/EH domain interactions is sufficient to impair recycling, a phenotype previously attributed to EHD in total (Naslavsky *et al*., 2004). One of the endocytosis-deficient *C. elegans* RME-1 mutants carried a mutation in the nucleotide P-loop located within the N terminus of all EHD proteins (Grant *et al*., 2001), suggesting that either disrupted nucleotide binding leads to recycling impairments independent from EH domain functions or that nucleotide binding influences EH domain functions. We thus tested whether nucleotide binding could modulate EH domain interactions by performing a series of coimmunoprecipitation studies with cell lysates that were preincubated without nucleotide addition, with ATP, with AMP, with ATPγS or ADPβS (Figure 10, A and B). FLAG-mRme-1/EHD1 was immunoprecipitated equally well under all of these conditions (Figure 10B). GFP-syndapin II-l specifically coimmunoprecipitated with FLAG-mRme-1/EHD1 (Figure 10A). The coimmunoprecipitation was dependent on the

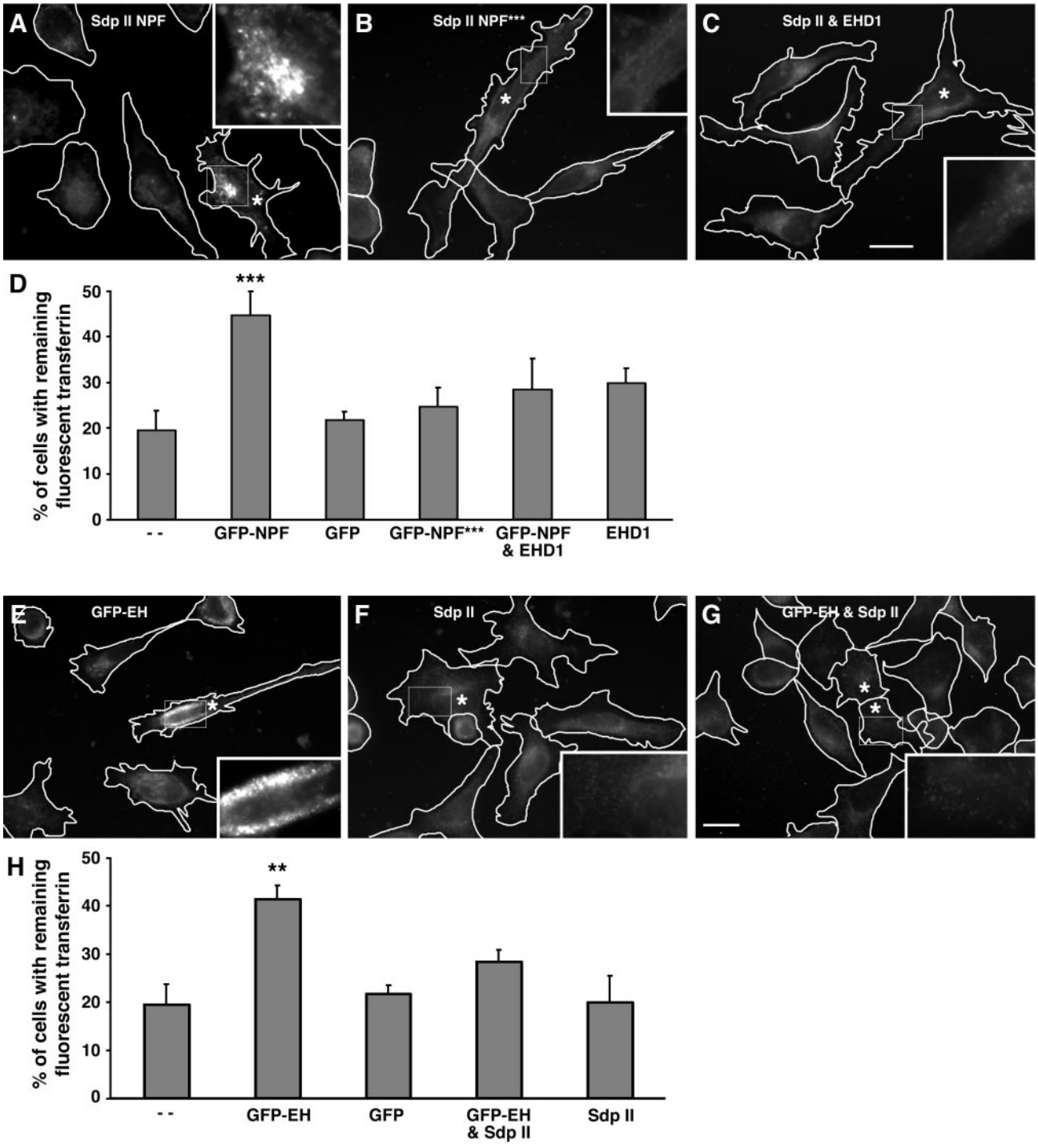

Figure 9. Interfering with EH domain/NPF motif interactions inhibits transferrin recycling and can be rescued by co-overexpression of the corresponding full-length proteins. (A–D) Interference with the syndapin/EHD1 interaction via GFP-syndapin II-l NPF overexpression and rescue by EHD1 co-overexpression in HeLa cells. (A–C) Pulse chase experiments with fluorescently labeled transferrin in cells overexpressing GFP-syndapin II-l NPF region (A), the corresponding triple NPF to NPV mutant (GFP-NPF***) (B) and a combination of GFP-syndapin II-l NPF and FLAG-EHD1 (C). (D) Quantitative data of scoring at least ~100 transfected cells per coverslip on six to 12 coverslips of five to eight independent assays. Transfected cells scored, GFP-NPF, 1489; GFP, 1268; GFP-NPF***, 1064; GFP-NPF and EDH1, 688; EHD1, 646. Error bars represent SEM. ***p value < 0.0001 (Fisher's PLSD). (E-H) Interference with the syndapin/EHD1 interaction via the EH domain of EHD1 and rescue by syndapin II-l. (E–G) Pulse chase experiments with fluorescently labeled transferrin in cells overexpressing GFP-EHD1 EH domain (E), FLAG-syndapin II-l (F) and a combination of GFP-EHD1 EH domain and FLAG-syndapin II-l (G). (H) Quantitative determination as in D. Transfected cells scored, GFP-EH, 865; FLAG- and Xpress-syndapin II-l, 535; GFP-EH and FLAG-syndapin II-l, 504. Error bars represent SEM of at least ~100 transfected cells on five to 12 coverslips of four to six independent assays. **p value = 0.0021. Cell borders of untransfected and transfected cells (marked by asterisks) are outlined. Insets in A–C and E–G are threefold enlargements of boxed areas in the corresponding images. Bars in C (for A–C) and in G (for E–G), 20 μm.

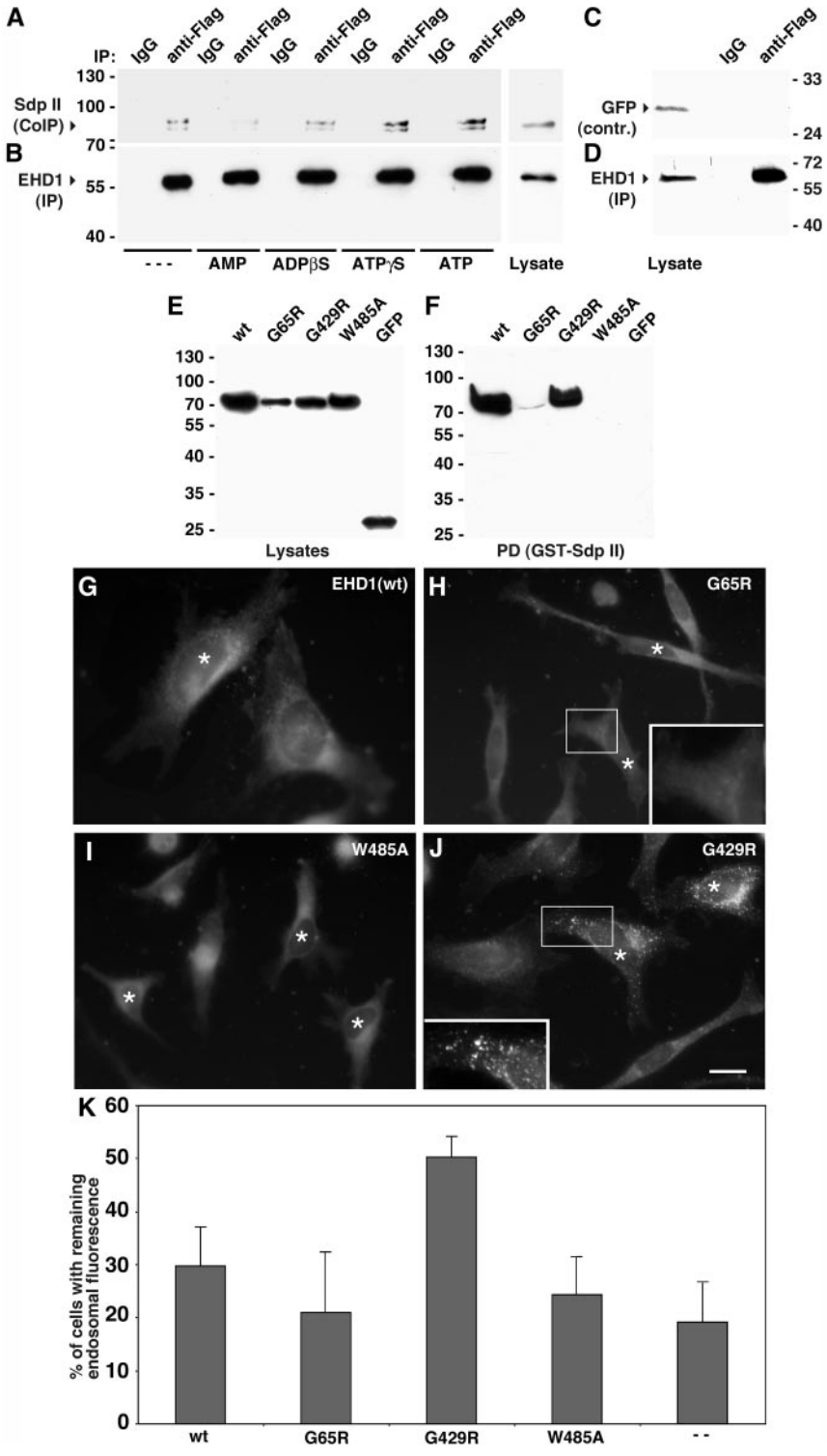

Figure 10. Nucleotide binding of EHD1 modulates interactions of the EH domain, which are crucial for receptor recycling. (A–D) Coimmunoprecipitation of GFP-syndapin II-l (A) but not GFP (C) with FLAG-EHD1 (B and D) from HEK293 cell lysates, which were preincubated for 10 min at room temperature without addition of nucleotides (—) or with addition of AMP, ADPβS, ATPγS, or ATP (5 mM final), by anti-FLAG antibodies covalently attached to protein G-Sepharose. The specific coimmunoprecipitation of GFP-SdpII-l was influenced by the preincubation with different nucleotides, as shown by anti-GFP immunoblotting (A). Quantitation of the bands of immunoprecipitated FLAG-EHD1 (with the use of the program Quantity One from Bio-Rad, Hercules, CA) confirmed the approximately equal efficiency of the immunoprecipitation. Quantitation of coimmunoprecipitated GFP-syndapin II-l and background subtraction yielded the following data: AMP, 22%; ADPβS, 50%; ATPγS, 105%; ATP, 130% of the value for no nucleotide addition (100%). (E and F) Affinity purification experiments of different GFP-EHD1 mutants expressed in HEK293 cells by immobilized GST-syndapin II-l. Analyses of lysates (E) and precipitated material (F) by anti-FLAG immunoblotting show that syndapin II-l coprecipitated wild-type EHD1 and EHD1 G429R but not the P-loop mutant G65R and the EH domain mutant W485A. (G–J) Analyses of fluorescently labeled transferrin after a chase of 20 min in untransfected HeLa cells (unmarked cells in G–J) and in cells overexpressing wild-type FLAG-EHD1 (G) and FLAG-EHD1 mutants (H, G65R; I, W485A; J, G429R). Transfected cells are marked by asterisks. Insets represent enlargements of boxed areas. Bar, 20 μm. (K) Quantitation of cells with remaining endosomal transferrin signal in percentage. Examined cells were from several independent transferrin recycling assays and analyzed by several independent investigators. Cells scored, untransfected cells, 350; wild-type EHD1 646; EHD1 G65R, 602; EHD1 G429R, 805; EHD1 W485A, 706. Error bars represent SEM.

syndapin part of the GFP-fusion protein because coexpressed GFP did not coimmunoprecipitate (Figure 10C) with FLAG-mRme1/EHD1 immunoprecipitated by anti-FLAG antibodies (Figure 10D). The amounts of GFP-syndapin II-l coimmunoprecipitated differed clearly under the five conditions applied (Figure 10). The addition of ATP or ATPγS supported the interaction but ADPβS and especially AMP suppressed it. Comparing several independent experiments, the amounts of GFP-syndapin II-l coimmunoprecipitated upon ATP or ATPγS addition were always higher or comparable with those performed under similar conditions without addition of nucleotides, and much higher than those obtained after AMP or ADPβS preincubation (Figure 10A). These coimmunoprecipitation experiments, however, did not exclude the possibility that the observed nucleotide effects were indirect or even EHD independent.

To demonstrate that nucleotide binding of mRme-1/EHD1 modulates the EH domain interaction with syndapin, we performed coprecipitation analyses with immobilized syndapin II-l and HEK293 cell lysates containing wild-type GFP-mRme-1/EHD1 and different mutants. GFP-mRme-1/EHD1 G65R represents a mutant in analogy to a dominant Rme-1 mutant isolated in mutational analyses of membrane trafficking in *C. elegans* (Grant *et al*., 2001). The G65R exchange is located in the nucleotide binding P-loop. We hypothesized that if the N-terminal nucleotide binding domain indeed influences syndapin's association with the C-terminal EH domain, then silencing the nucleotide binding domain by mutation may interfere with syndapin binding. As a control for interfering with EH domain-dependent syndapin binding, we additionally assayed a mutant of mRme-1/EHD1 with a disrupted EH domain (GFP-mRme-1/EHD1 W485A) that was constructed based on structural data for the Eps15 EH domain 2 (de Beer *et al*., 2000). Additionally, we included GFP-mRme-1/EHD1 G429R, the mammalian version of a second *C. elegans* Rme-1 dominant mutant. Overexpression of mRme-1/EHD1 G429R has been observed to block recycling in several recent studies (Lin *et al*., 2001; Caplan *et al*., 2002; Picciano *et al*., 2003; Park *et al*., 2004). The molecular mechanisms by which the G429R mutation brings about this effect are unknown.

We observed that the G65R mutant was strongly deficient for syndapin binding (Figure 10, E and F). The immunosignal obtained from the eluates was almost as weak as that of the EH domain mutant that served as a negative control and that lacked all specific syndapin binding activity. In contrast, the G429R mutant showed a strong syndapin binding and did not differ significantly from wild-type mRme-1/EHD1 under affinity purification conditions (Figure 10F).

EHD Mutants Defective in Syndapin Binding Do Not Act Dominant Negatively on Receptor Recycling

We have demonstrated that overexpression of the syndapin-binding EH domain of mRme-1/EHD1 alone has a dominant-negative effect on transferrin recycling (Figure 9). Lin *et al*. (2001) showed that overexpression of the G65R mutant did not cause any impairment. We hypothesized that the lack of G65R-induced recycling defects is due to the observed strongly decreased syndapin binding activity of G65R mutants (Figure 10, H and F). If this hypothesis is correct, then overexpression of the EH domain mutant (W485A) also should lack dominant-negative activity. Indeed, the W485A mutant did not cause an inhibition in recycling (Figure 10, I and K) compared with overexpression of the G65R mutant (Figure 10, H and K) or to untransfected cells (Figure 10K). In contrast, about one-half of all G429R-overexpressing cells showed significant remaining transferrin (Figure 10, J and K). Overexpression of a wild-type, i.e., presumably fully functional, mRme-1/EHD1, only caused extremely mild, if any, effects on transferrin recycling (Figure 10G). Quantitation of the effects elicited showed that only 30% of the mRme-1/EHD1–overexpressing cells were transferrin positive (Figure 10K). This is consistent with a previously reported lack of inhibition of transferrin recycling (Lin *et al*., 2001). Also, recycling of a major histocompatibility complexes component and AMPA receptors was rather enhanced than inhibited (Caplan *et al*., 2002; Park *et al*., 2004). In summary, our analysis of the different syndapin and mRme-1/EHD1 point mutants and deletion constructs revealed the critical importance of EH domain/NPF interactions for the receptor recycling process, because only proteins capable to interfere with these interactions disrupt this cellular process.

DISCUSSION

Syndapins have been proposed to interconnect vesicle formation in receptor-mediated endocytosis and the cortical actin cytoskeleton (Qualmann and Kessels, 2002). Our new data indicate that syndapins are parts of a more general mechanism in membrane trafficking, because they interact with EHD proteins that function in exit from the endosomal recycling compartment. Syndapin I, syndapin II-s, and syndapin II-l but not syndapin III interact with EHD proteins. The interaction is based on associations of the EH domain of EHD proteins with syndapin NPF motifs, as we demonstrated by yeast two-hybrid analysis, affinity purifications, and in vivo reconstitution of EHD/syndapin complexes. The interaction is direct, as proven by blot overlay studies. These findings are consistent with data Xu *et al*. (2004) reported while this manuscript was in preparation. They showed by biochemical methods that a C-terminal part of syndapin II that encompasses the region, which contains the NPF motifs, interacts with the EH domain of EHD1 in vitro (Xu *et al*., 2004). Our mutational analyses prove that the interaction indeed requires NPF motifs. Consistently, syndapin III, which does not exhibit NPF motifs, did not bind to EHD proteins. Additionally, our mutational analyses revealed that NPF 364-6 is the most important EHD-binding motif in syndapin II. This region is alternatively spliced and is absent in the short versions of syndapin II (Qualmann and Kelly, 2000). EHD proteins therefore not only represent the first differential in vivo binding partners for the three syndapin isoforms but also can differentiate between the long and short splice variants of syndapin II.

All syndapin NPF motifs except for one in syndapin I are preceded by one or even two (syndapin II NPF 364-6) serines. The positions and numbers of serines may correlate with the strength of interaction, as proposed for other EH domains (Salcini *et al*., 1997). Our data demonstrate that syndapin EH domain interactions are specific for EHD proteins. Eps15 EH domains were shown to prefer basic or hydrophobic amino acids C-terminal of the NPFs (Salcini *et al*., 1997). In contrast, the NPFs of syndapins are directly followed by acidic or polar residues. We propose that these NPF-context differences determine the specificity for EHD proteins.

Careful comparative analyses of the EH domains of EHD proteins, intersectin, and Eps15 and correlations with structural studies performed for the second Eps15 EH domain (de Beer *et al*., 2000) additionally reveal the molecular determinants within the EH domain that are likely to bring about the specificity of syndapins for EHD proteins (Figure S4). Four positions, which are strictly conserved among EHD proteins, differ significantly from the intersectin and the Eps15 EH domains. These include the position corresponding to E163, which is a serine or threonine in all EHD proteins, and E170, which is a lysine in all EHD proteins (Figure S4). Because both of these positions have been identified as residues involved in the recognition and specificity control at the +3 position, i.e., the amino acid C terminal of the NPF, in the structural analysis of the second Eps15 EH domain bound to the NPF-containing Hrb peptide (de Beer *et al*., 2000), they may help in generating the specificity differences observed between EHD protein EH domains and those of Eps15 and intersectin. It seems likely that the highly conserved lysine in the E170 position directly contacts the negatively charged amino acids C-terminal of almost all syndapin NPFs.

However, these two differences in primary sequence cannot explain the inability of EHD2 to bind syndapins, because

these two residues are conserved among all EHD proteins, including the *C. elegans* ortholog. Interestingly, our analyses revealed two additional positions that differ from Eps15 and intersectin EH domains but are strongly conserved among EHD proteins except in the EHD2 isoform, V154 and M203. The M203 position is taken by an asparagine or lysine in EHD1, 3, and 4 and in the *C. elegans* protein but is a serine in EHD2. M203 has been shown to be in direct contact with the leucine after the NPF motif in the Hrb peptide studied in complex with the second Eps15 EH domain (de Beer *et al*., 2000). The asparagine and the lysine in EHD1, 3, and 4 (Figure S4) may, by analogy, contact the glutamate or aspartate, which usually follows the syndapin NPFs (Figure 2G). The second position that is likely to explain the observed differential binding of EHD proteins corresponds to V154 and is strictly hydrophobic in Eps15 and intersectin EH domains. It is exchanged for a glutamate in EHD1, 3, and 4 but is a tryptophane in EHD2. This residue is a direct neighbor of L155 shown to be a highly conserved part of the NPF binding pocket (de Beer *et al*., 2000).

Syndapins are new interaction partners of EHD proteins that were previously strongly suggested to function in the early uptake stages in the endocytic pathway (Kessels and Qualmann, 2004). Additionally, syndapins seem to play a role in vesicle formation from Golgi membranes (Kessels *et al*., 2003). The interaction with EHD proteins also may implicate them in vesicle formation from endosomal membranes. We thus propose that syndapins are part of a machinery widely used for vesicle formation processes from several different cellular membranes, like other well known trafficking proteins such as clathrin and dynamin.

Naslavsky *et al*. (2004) reported on an interaction of EHD1 with the rab4/rab5 effector rabenosyn 5 in vitro. Rabenosyn 5 RNAi caused a block in the endocytic pathway upstream of EHD proteins, probably during passage through early endosomes (Naslavsky *et al*., 2004), a role of rabenosyn already suggested by previous observations (de Renzis *et al*., 2002). This does not exclude the possibility that rabenosyn 5 also functions later in the endocytic pathway. However, these functions downstream of its crucial role cannot be addressed by interfering with the protein level in general. Similarly, it was impossible to address the involvement of syndapins in later steps of the endocytic pathway, as implicated by their interaction with EHD proteins, via interference with syndapins in toto. The inhibition of the internalization step upon introduction of anti-syndapin antibodies in vivo strongly suggested that syndapins are already critical for a step very early in the endocytic process. The inhibition of endocytic internalization by antibodies directed against the SH3 domain-containing C terminus of syndapins observed is consistent with our previous examinations. Syndapin I and II interact with dynamins, and an excess of their dynamin binding SH3 domain interferes with the dynamin-dependent step in vesicle formation in vitro and in vivo (Simpson *et al*., 1999; Qualmann and Kelly, 2000). Interfering with syndapin SH3 domain functions by overexpression of the syndapin binding interface of N-WASP also blocked endocytosis and could be rescued by co-overexpression of full-length syndapin I or syndapin II (Kessels and Qualmann, 2002).

Our current analyses, however, revealed that the syndapin region involved in EHD interaction is distinct from the SH3 domain. Manipulation of this interface allowed us to identify an involvement of syndapin function in later steps in the endocytic recycling pathway, in the endocytic recycling step, by disrupting specifically EH domain/NPF motif interactions and leaving syndapin SH3 domain functions untouched. The NPF region of syndapin II-l had a strong impact on transferrin receptor recycling, when uncoupled from functions of other syndapin domains. The NPF specificity of this effect was demonstrated by the triple NPF to NPV mutant, which did not block recycling. Importantly, we were able to rescue the NPF-induced inhibition by co-overexpression of mRme-1/EHD1 showing that the interference with EHD protein functions was the primary cause of the effect. This strongly suggests that the capability of EHD proteins to undergo EH domain interactions with NPF-containing proteins, such as syndapins, is crucial for recycling.

The fact that NPF-containing binding partners of EHD proteins also participate in endosomal recycling is highlighted by the fact that uncoupling the EH domain from the rest of mRme-1/EHD1 strongly impaired transferrin recycling as well. Our analyses revealed that the recycling inhibition caused by the syndapin NPF region or the EH domain of mRme-1/EHD1 is comparable with that of the known dominantly interfering mRme-1/EHD1 mutant G429R (Lin *et al*., 2001). Because the association of mRme-1/EHD1 G429R with endosomes (Lin *et al*., 2001), its oligomerization as well as its capability to bind and hydrolyze ATP are intact (Lee *et al*., 2005) and we showed that mRme-1/EHD1 G429R still associates with syndapins, the molecular basis for this dominant interference remains unclear. The dominant-negative effect of the EH domain strongly supports our conclusion that specifically EH domain/NPF motif interactions are required for endosomal recycling and that one likely reason for the inhibition of the endocytic pathway observed upon suppression of mRme-1/EHD1 levels by gene disruption (Grant *et al*., 2001) or RNAi (Naslavsky *et al*., 2004) is the inability of such cells to make the required EH domain-dependent interconnections with NPF motif-containing, specific EHD protein interaction partners, such as syndapins. Consistently, the recycling defect caused by overexpression of the EH domain of mRme-1/EHD1 can be rescued by coexpression of syndapin II.

Our analyses provide an explanation for the finding that overexpression of mRme-1/EHD1 G65R did not cause any inhibition in recycling (Lin *et al*., 2001; this study). Our protein interaction studies strongly suggest that this lack of dominant-negative properties reflects the lack of EH domain function; G65R mutants were not able to associate with syndapins (Figure 10). The analog mutation in the *C. elegans* protein disrupted dimerization of ceRme-1 (Lee *et al*., 2005). Provided that the mRme-1/EHD1 mutant G65R behaves similarly, overexpression of G65R mRme-1/EHD1 would neither sequester endogenous EHD proteins into dimers with the mutant protein nor interfere with endogenous EH domain/NPF interactions critical for recycling.

G65R mutants exhibit a disrupted P-loop, and we found that there is some functional cross-talk of the nucleotide binding of the mRme-1/EHD1 N-terminal domain and the C-terminal EH domain interacting with syndapins. This result of our mutational analyses also is supported by the observed changes in syndapin binding to wild-type mRme-1/EHD1 in vivo when incubations with ATP, ADP, AMP, and nonhydrolysable derivatives, respectively, were performed. mRme-1/EHD1 has recently been shown to be a slow ATPase (Lee *et al*., 2005). EH domain interactions with syndapins seem to be suppressed under conditions that reduce ATP binding or in a mutant protein where nucleotide binding is disrupted completely. It thus seems possible that the ATPase domain of mRme-1/EHD1 is in control of the EH domain interactions with NPF motif-containing proteins

that we have revealed to be crucial for an efficient recycling of receptors back to the plasma membrane.

In the G429R mutant, in contrast, the EH domain seems functional, because it bound syndapins very well, yet the protein has strong dominant-negative effects on recycling because this mutation obviously causes some nonfunctionality elsewhere in the molecule (Lin *et al*., 2001; this study). The G429R mutant is strongly localized to endosomes (Lin *et al*., 2001). Strong syndapin interactions with the G429R mutant at these membranes and the resulting partial sequestration of endogenous syndapins away from the endocytic vesicle formation machinery at the plasma membrane may be one reason for the observed slight impairment of endocytosis in G429R mutant-overexpressing cells (Figure S3).

One possible mechanistic role of syndapins in exit from the ERC is that they may orchestrate a dynamic interplay of EHD proteins with activators of the actin nucleation machinery and/or further components involved in membrane trafficking in analogy to their proposed function during endocytic vesicle formation (Qualmann and Kessels, 2002; Kessels and Qualmann, 2004). This putative role would require that syndapins interact with multiple interaction partners simultaneously. Because the EHD protein interaction involves the syndapin NPF motifs and all other interactions described are mediated via the SH3 domain (Kessels and Qualmann, 2004), it seems very possible that one syndapin molecule can serve as physical link between EHD proteins and further interaction partners. Additionally, we have discovered that syndapins dimerize in a non-SH3 domain-dependent manner (Kessels and Qualmann, unpublished data). The observed clustering of EH domain-coated mitochondria upon co-overexpression of both syndapin II full-length as well as of syndapin II ΔSH3 (Figure 7) indicates that also dimerization and NPF-interactions can occur simultaneously. This is further supported by the fact that dimerization is indeed independent of the NPF region (Kessels and Qualmann, unpublished data). Syndapin dimerization strongly increases the number of possible interconnections originating from syndapin/EHD protein complexes and may therefore represent a molecular basis for the formation of multivalent, dynamic scaffolds during vesicle formation not only at the plasma membrane but also at membranes of the ERC.

In neurons, the accumulation of both EHD proteins and syndapin in perinuclear regions as well as in synaptic areas suggests that EHD protein/syndapin complexes are involved in recycling in the cell soma but also within the very small subcellular compartment of the synapse. This is supported by our subcellular fractionation data. Syndapins seem to occur both pre- and postsynaptically, as suggested by colocalizations with the synaptic vesicle protein synaptophysin (Qualmann *et al*., 1999) and our transfections of primary hippocampal neurons. EHD proteins seem to have a very similar distribution. The existence of a postsynaptic pool of EHD proteins is supported by our colocalization experiments in transfected neurons and is in line with a recent report showing that affecting EHD protein functions and/or interactions via overexpression of GFP-EHD1 G429R impairs the recycling of postsynaptic AMPA-type glutamate receptors (Park *et al*., 2004). The endocytosis of AMPA receptors also involves the syndapin binding partner dynamin (Carroll *et al*., 1999). It therefore seems likely that molecular interconnections mediated by syndapins play important roles in both the endocytosis and the recycling of AMPA-type glutamate receptors—processes that are thought to represent a mechanism for synaptic plasticity—and thereby for learning and memory formation.

ACKNOWLEDGMENTS

We thank Kathrin Hartung and Sabine Opitz for excellent technical assistance and Prof. Dr. Eckart D. Gundelfinger for support. We thank Wibke Leibig and Kathrin Hartung for inserting GFP into the mitochondrial targeting vector, Oliver Kobler for help with the confocal microscopy, and Akvile Inciute for help with the neuronal cultures. We are particularly grateful to Wolfgang Tischmeyer for the help with statistical analyses and to Brian Kay for the plasmids encoding GST-Eps15 EH and GST-Intersectin EH domains. This work was supported by a La Caixa/Deutschen Akademischen Austauschdienst fellowship (to R. P.) and National Institutes of Health Grant GM-67237-01 (to B.D.G.) and the Kultusministerium Land Sachsen-Anhalt 3199A/0020G (to B. Q.) as well as by Deutsche Forschungsgemeinschaft Grants Qu 116/2-1, Qu 116/2-3, and Ke 685/2-1 (to B. Q. and M.M.K.).

REFERENCES

Caplan, S., Naslavsky, N., Hartnell, L. M., Lodge, R., Polishchuk, R. S., Donaldson, J. G., and Bonifacino, J. S. (2002). A tubular EHD1-containing compartment involved in the recycling of major histocompatibility complex class I molecules to the plasma membrane. EMBO J. *21*, 2557–2567.

Carroll, R. C., Beattie, E. C., Xia, H., Luscher, C., Altschuler, Y., Nicoll, R. A., Malenka, R. C., and von Zastrow, M. (1999). Dynamin-dependent endocytosis of ionotropic glutamate receptors. Proc. Natl. Acad. Sci. USA *96*, 14112–14117.

Chen, W., Feng, Y., Chen, D., and Wandinger-Ness, A. (1998). Rab11 is required for trans-Golgi network-to-plasma membrane transport and a preferential target for GDP dissociation inhibitor. Mol. Biol. Cell. *9*, 3241–3257.

de Beer, T., Hoofnagle, A. N., Enmon, J. L., Bowers, R. C., Yamabhai, M., Kay, B. K., and Overduin, M. (2000). Molecular mechanism of NPF recognition by EH domains. Nat. Struct. Biol. *7*, 1018–1022.

de Renzis, S., Sonnichsen, B., and Zerial, M. (2002). Divalent Rab effectors regulate the sub-compartmental organization and sorting of early endosomes. Nat. Cell Biol. *4*, 124–133.

Galperin, E., Benjamin, S., Rapaport, D., Rotem-Yehudar, R., Tolchinsky, S., and Horowitz, M. (2002). EHD *3*, a protein that resides in recycling tubular and vesicular membrane structures and interacts with EHD1. Traffic *3*, 575–589.

Grant, B., Zhang, Y., Paupard, M. C., Lin, S. X., Hall, D. H., and Hirsh, D. (2001). Evidence that RME-1, a conserved C. elegans EH-domain protein, functions in endocytic recycling. Nat. Cell Biol. *3*, 573–579.

Kessels, M. M., Dong, J., Westermann, P., and Qualmann, B. (2003). Dynamin II and syndapin II form heterodimeric complexes promoting vesicle formation at the trans-Golgi network. Mol. Biol. Cell *14* (Suppl.) 337a (Abstract #2111).

Kessels, M. M., Engqvist-Goldstein, Å.E.Y., and Drubin, D. G. (2000). Association of mouse actin-binding protein 1 (mAbp1/SH3P7), an Src kinase target, with dynamic regions of the cortical actin cytoskeleton in response to Rac1 activation. Mol. Biol. Cell *11*, 393–412.

Kessels, M. M., Engqvist-Goldstein, A. E., Drubin, D. G., and Qualmann, B. (2001). Mammalian Abp1, a signal-responsive F-actin-binding protein, links the actin cytoskeleton to endocytosis via the GTPase dynamin. J. Cell Biol. *153*, 351–366.

Kessels, M. M., and Qualmann, B. (2002). Syndapins integrate N-WASP in receptor-mediated endocytosis. EMBO J. *21*, 6083–6094.

Kessels, M. M., and Qualmann, B. (2004). The syndapin protein family: linking membrane trafficking with the cytoskeleton. J. Cell Sci. *117*, 3077–3086.

Lee, D. W., Zhao, X., Scarselletta, S., Schweinsberg, P. J., Eisenberg, E., Grant, B. D., and Greene, L. E. (2005). Interaction of RME-1/EHD1 with nucleotide. J. Biol. Chem. *280*, 17213–17220.

Lin, S. X., Grant, B., Hirsh, D., and Maxfield, F. R. (2001). Rme-1 regulates the distribution and function of the endocytic recycling compartment in mammalian cells. Nat. Cell Biol. *3*, 567–572.

Maxfield, F. R., and McGraw, T. E. (2004). Endocytic recycling. Nat. Rev. Mol. Cell. Biol. *5*, 121–132.

Merrifield, C. J., Feldman, M. E., Wan, L., and Almers, W. (2002). Imaging actin and dynamin recruitment during invagination of single clathrin-coated pits. Nat. Cell Biol. *4*, 691–698.

Merrifield, C. J., Qualmann, B., Kessels, M. M., and Almers, W. (2004). Neural Wiskott Aldrich Syndrome Protein (N-WASP) and the Arp2/3 complex are recruited to sites of clathrin-mediated endocytosis in cultured fibroblasts. Eur. J. Cell Biol. *83*, 13–18.

Mintz, L., Galperin, E., Pasmanik-Chor, M., Tulzinsky, S., Bromberg, Y., Kozak, C. A., Joyner, A., Fein, A., and Horowitz, M. (1999). EHD1–an EH-domain-containing protein with a specific expression pattern. Genomics *59*, 66–76.

Naslavsky, N., Boehm, M., Backlund, P. S., Jr., and Caplan, S. (2004). Rabenosyn-5 and EHD1 interact and sequentially regulate protein recycling to the plasma membrane. Mol. Biol. Cell *15*, 2410–2422.

Park, M., Penick, E. C., Edwards, J. G., Kauer, J. A., and Ehlers, M. D. (2004). Recycling endosomes supply AMPA receptors for LTP. Science *305*, 1972–1975.

Picciano, J. A., Ameen, N., Grant, B. D., and Bradbury, N. A. (2003). Rme-1 regulates the recycling of the cystic fibrosis transmembrane conductance regulator. Am. J. Physiol. *285*, C1009–C1018.

Pohl, U., Smith, J. S., Tachibana, I., Ueki, K., Lee, H. K., Ramaswamy, S., Wu, Q., Mohrenweiser, H. W., Jenkins, R. B., and Louis, D. N. (2000). EHD2, EHD3, and EHD4 encode novel members of a highly conserved family of EH domain-containing proteins. Genomics *63*, 255–262.

Qualmann, B., Boeckers, T. M., Jeromin, M., Gundelfinger, E. D., and Kessels, M. M. (2004). Linkage of the actin cytoskeleton to the postsynaptic density via direct interactions of Abp1 with the ProSAP/Shank family. J. Neurosci. *24*, 2481–2495.

Qualmann, B., and Kelly, R. B. (2000). Syndapin isoforms participate in receptor-mediated endocytosis and actin organization. J. Cell Biol. *148*, 1047–1062.

Qualmann, B., and Kessels, M. M. (2002). Endocytosis and the cytoskeleton. Int. Rev. Cytol. *220*, 93–144.

Qualmann, B., Kessels, M. M., and Kelly, R. B. (2000). Molecular links between endocytosis and the actin cytoskeleton. J. Cell Biol. *150*, F111–F116.

Qualmann, B., Roos, J., DiGregorio, P. J., and Kelly, R. B. (1999). Syndapin I, a synaptic dynamin-binding protein that associates with the neural Wiskott-Aldrich syndrome protein. Mol. Biol. Cell *10*, 501–513.

Ren, M., Xu, G., Zeng, J., De Lemos-Chiarandini, C., Adesnik, M., and Sabatini, D. D. (1998). Hydrolysis of GTP on rab11 is required for the direct delivery of transferrin from the pericentriolar recycling compartment to the cell surface but not from sorting endosomes. Proc. Natl. Acad. Sci. USA *95*, 6187–6192.

Salcini, A. E., Confalonieri, S., Doria, M., Santolini, E., Tassi, E., Minenkova, O., Cesareni, G., Pelicci, P. G., and Di Fiore, P. P. (1997). Binding specificity and in vivo targets of the EH domain, a novel protein-protein interaction module. Genes Dev. *11*, 2239–2249.

Schneider, C., Newman, R. A., Sutherland, D. R., Asser, U., and Greaves, M. F. (1982). A one-step purification of membrane proteins using a high efficiency immunomatrix. J. Biol. Chem. *257*, 10766–10769.

Seidenbecher, C. I., *et al*. (2004). Caldendrin but not calmodulin binds to light chain 3 of MAP1A/B: an association with the microtubule cytoskeleton highlighting exclusive binding partners for neuronal Ca(2+)-sensor proteins. J. Mol. Biol. *336*, 957–970.

Simpson, F., Hussain, N. K., Qualmann, B., Kelly, R. B., Kay, B. K., McPherson, P. S., and Schmid, S. L. (1999). SH3-domain-containing proteins function at distinct steps in clathrin-coated vesicle formation. Nat. Cell Biol. *1*, 119–124.

Slepnev, V. I., and De Camilli, P. (2000). Accessory factors in clathrin-dependent synaptic vesicle endocytosis. Nat. Rev. Neurosci. *1*, 161–172.

Stoorvogel, W., Oorschot, V., and Geuze, H. J. (1996). A novel class of clathrin-coated vesicles budding from endosomes. J. Cell Biol. *132*, 21–33.

van Dam, E. M., Ten Broeke, T., Jansen, K., Spijkers, P., and Stoorvogel, W. (2002). Endocytosed transferrin receptors recycle via distinct dynamin and phosphatidylinositol 3-kinase-dependent pathways. J. Biol. Chem. *277*, 48876–48883.

Xu, Y., Shi, H., Wei, S., Wong, S. H., and Hong, W. (2004). Mutually exclusive interactions of EHD1 with GS32 and syndapin II. Mol. Membr. Biol. *21*, 269–277.